JOURNAL OF GEOPHYSICAL RESEARCH, VOL. 111, F04014, doi:10.1029/2006JF000583, 2006

Click Here for Full Article

Erosion by rivers and transport pathways in the ocean: A provenance tool using ^{40}Ar-^{39}Ar incremental heating on fine-grained sediment

Sam VanLaningham,[1] Robert A. Duncan,[1] and Nicklas G. Pisias[1]

Received 23 May 2006; accepted 8 September 2006; published 27 December 2006.

[1] We use ^{40}Ar-^{39}Ar incremental heating to fingerprint bulk fluvial sediment entering the northeast Pacific Ocean, with the long-term intent of tracking sediment source and transport changes from the terrestrial system to the marine environment through time. We show reproducible age spectra from individual rivers accounting for the majority of sediment delivered to the Pacific margin. Two tests are performed to confirm the validity of the bulk sediment ^{40}Ar-^{39}Ar incremental heating measurements and to address why polymineralic sediment might yield concordant age steps. The first model tests, in light of bulk mineralogy and diffusion of Ar from silicates, whether measured K/Ca spectra (measured from ^{39}Ar and ^{37}Ar, respectively) are consistent with typical values for K- and Ca-bearing minerals. Calculations show that the bulk mineralogy is reflected in the outgassing K/Ca spectra and identify plagioclase as the dominant mineral contributing to the plateau-defining portion of the age spectra. A second model predicts bulk sediment ages from integrated bedrock cooling age-area estimates in order to examine whether bulk sediment plateau ages are representative of the average cooling age of rocks from a given river basin. Calculated and observed ages are notably similar in three river basins when topographic and lithologic effects are accounted for. Overall, this technique shows considerable promise, not only in tracking individual terrigenous sources in the marine realm but also for understanding processes such as erosion and sediment transport in terrestrial systems.

Citation: VanLaningham, S., R. A. Duncan, and N. G. Pisias (2006), Erosion by rivers and transport pathways in the ocean: A provenance tool using ^{40}Ar-^{39}Ar incremental heating on fine-grained sediment, *J. Geophys. Res.*, *111*, F04014, doi:10.1029/2006JF000583.

1. Introduction

[2] Deep-sea sediments provide a particularly complete and integrated record of Earth's climate and tectonic systems. To fully appreciate information contained in the terrigenous fraction of marine sediments, that fraction derived from continental erosion, it is critical that we are able to identify the source regions and transport pathways of the sediment deposited at any given location. With this "provenance" information we can better delineate a variety of processes including the response of ocean circulation and continental landscapes to climate change, as well as tectonic processes that modify the morphology of the landscape.

[3] A variety of studies have illustrated the power of using terrigenous material to understand dynamics of Earth's climate system. For example, changes in oceanographic circulation over glacial-interglacial timescales have been discovered in many regions of the world through identification of terrigenous sources and their distribution in the sediment record [*Fagel et al.*, 1996, 2002; *Jantschik and Huon*, 1992; *Walter et al.*, 2000]. Patterns of sea-ice movement have been resolved by tracking entrained Fe oxides from their original, terrestrial source [*Darby*, 2003]. Spatially and temporally variable precipitation patterns in the coastal Chilean and Andean mountains have been better understood over the last 28,000 years through terrigenous Fe changes seen in offshore sediment cores [*Lamy et al.*, 1999], while characterizing the provenance and pathways of ice bergs in the northeast Atlantic have been carried out by studies of ice-rafted and glacial debris using ^{40}Ar-^{39}Ar dating methods applied to detrital hornblendes and sediments [*Hemming et al.*, 1998, 2002]. Identifying the cratonic sources of glacial till via large populations of single crystal ^{40}Ar-^{39}Ar total fusion ages has been a recent avenue for provenance study related to natural climate variations (M. Roy et al., Constraints on a long-lived Keewatin ice dome from ^{40}Ar/^{39}Ar dating of mineral grains from mid-continent glacial deposits, manuscript in preparation, 2006).

[4] Beyond the paleoclimate world, a variety of tectonic processes have also been unraveled through provenance studies of river sediments [*Bernet et al.*, 2004; *Carrapa et al.*, 2004; *Clift et al.*, 2001, 2002; *Garzanti et al.*, 1996, 2005; *Reiners et al.*, 2005a; *Spiegel et al.*, 2004; *Wobus et al.*, 2003], while linking and deconvolving climatic and tectonic signals is at the forefront of studies of Earth surface processes today [*Clift and Blusztajn*, 2005; *Kuhlemann et al.*, 2004].

[1] College of Oceanic and Atmospheric Sciences, Oregon State University, Corvallis, Oregon, USA.

Copyright 2006 by the American Geophysical Union.
0148-0227/06/2006JF000583$09.00

[5] The spatial resolution at which terrigenous sources can be identified is dependent on the diversity of the age, mineralogy and chemistry of rocks that are eroded and on the development of techniques that characterize those sources. Generally, provenance has been distinguished on the scale of geologic provinces [*Fagel et al.*, 2002; *Hemming et al.*, 1998; *Lamy et al.*, 1998, 1999; *Walter et al.*, 2000]. There have been fewer studies that fingerprint specific fluvial sediment sources via isotopic methods [*Clift et al.*, 2002, 2004] or mineralogic techniques [*Garzanti et al.*, 2005]. Since most rivers in a given region erode common rock types, it remains difficult to resolve provenance at the fluvial basin scale. Fission track studies [*Brandon and Vance*, 1992; *Carter*, 1999], U-Pb and (U-Th)/He dating of detrital zircons [*Reiners et al.*, 2005a] and a variety of single-grain K-feldspar [*Copeland et al.*, 1990] and mica analyses [*Carrapa et al.*, 2004; *Heller et al.*, 1992] have proven to be extremely powerful ways to resolve sediment source. However, the low abundances and very small particle sizes of minerals beyond the shelf-slope break make the applicability of these single-grain methods tenuous in the deeper marine realm. Yet the deep sea is where the most continuous sediment records are preserved, since sea level oscillations expose and erode the shelf. Moreover, terrigenous material makes up 77% of sediment in the world's oceans [*Lisitzin*, 1996], and yet detailed knowledge about the source of much of these sediments is lacking since so much of it is made up of very small particle sizes.

[6] In this paper we investigate the resolution at which ^{40}Ar-^{39}Ar incremental heating methods can characterize provenance of bulk fluvial, silt-sized sediments (20–63 μm). Bulk sediment ages using the ^{40}Ar-^{39}Ar system were previously reported by *Hemming et al.* [2002]. That work was part of a larger study that showed that the bulk sediment ages reflected terrestrial source, paving the way for this study. *Hemming et al.* [2002] did not explore the meaning of the age spectra, potential fluvial sources were not characterized and smaller size fractions were measured. Other ^{40}Ar-^{39}Ar incremental heating studies have been carried out on the clay-sized fraction of sediments, using a technique that overcomes problems related to Ar recoil and loss in fine-grained sediment [*Dong et al.*, 1995]. Although these methods can be invaluable in the marine setting [*Pettke et al.*, 2000], we focus on the silt-sized fraction so as to better ensure that we capture reproducible ages related to source rock cooling, avoiding ages that could be a function of weathering or diagenesis [*Dong et al.*, 1995].

[7] We apply ^{40}Ar-^{39}Ar incremental heating methods to characterize fluvially borne terrigenous material at its last juncture before entering the ocean, with the expectation of applying it as a robust provenance tracer in marine sediments. In this paper we show that concordant middle- to high-temperature step ages derived from this method reflect the average cooling age of the rocks that are eroded from exposed source rocks, as others have inferred [*Hemming et al.*, 2002; *Pettke et al.*, 2000]. Reproducible age spectra, including concordant step ages comprising a majority of the Ar release (termed plateaus) can be extracted from the bulk sediment, in many cases. This work also suggests that it may be possible to accurately identify specific sediment sources that derive from the same geologic province(s), but drain varying proportions thereof. We use K/Ca information to address questions about why sediments produce age plateaus and what minerals are likely characterizing the gas at different temperatures. We finish with simple calculations that evaluate how well the measured bulk sediment ^{40}Ar-^{39}Ar plateau ages represent the average cooling age of minerals from contributing rock types in a given river basin and discuss this technique's promise and limitations.

2. Expectations for ^{40}Ar-^{39}Ar Incremental Heating Experiments on Multiphase Detrital Sediments

[8] A ^{40}Ar-^{39}Ar total fusion (single step) age or K-Ar age documents the time at which a mineral, or whole rock cooled below a certain closure temperature (we use cooling age realizing that it is synonymous with crystallization age in volcanic rocks, but may be significantly younger in slowly cooled plutonic rocks). By using the incremental heating technique, valuable geologic information can be gained such as whether metamorphic, hydrothermal, or weathering events have affected the distribution of K and Ar in a mineral or whole rock sample. In essence, an incremental heating age spectrum (age vs. temperature or %gas released) can often reveal much of the thermal history of a mineral or whole rock. In this study we employ the incremental heating technique because of the information gained over a fusion age alone. For instance, since we extract gas from a fine-grained mixture of minerals from a variety of geologic provinces, the step heating information (both age and K/Ca) provides a way of determining the variety and relative contributions of minerals to the age patterns presented by the sediment samples. In the following section, we discuss the traditional features associated with ^{40}Ar-^{39}Ar age spectra so that there is a framework for understanding the methods and results from this study.

[9] In an age spectrum derived from incremental heating of a single mineral, the main interpretable features are cooling age, Ar loss, inherited or excess Ar, and Ar recoil. Cooling ages are often indicated by concordant step ages, forming a plateau (Figure 1a). Ar loss occurs from a variety of conditions such as reheating during metamorphic events, surface weathering, chemical alteration, and mechanical grinding (see summaries by *Dalrymple and Lanphere* [1969] and *McDougall and Harrison* [1999]). ^{40}Ar loss is evidenced by ever increasing ages in the low-temperature steps of the age spectrum (Figure 1b), presumably due to heating-activated diffusion from less retentive margins and fractures in crystals. Excess Ar, resulting from undegassed mantle-derived ^{40}Ar at the time of crystallization or hydrothermally deposited, nonatmospheric ^{40}Ar, is often detectable in ^{40}Ar-^{39}Ar age spectra, usually by a saddle-shaped degassing pattern; i.e., older than actual crystallization ages at low- and high-temperature steps.

[10] Ar recoil presents another problem. It results in ^{39}Ar and ^{37}Ar loss or relocation during irradiation, due to recoil of target atoms (K and Ca, respectively) during neutron capture [*Faure*, 1986; *Turner and Cadogan*, 1974]. When ^{39}Ar is lost from crystal margins during irradiation in the reactor, the ^{40}Ar/^{39}Ar ratio at low-temperature steps increases, and so does measured age. In fine-grained, multiphase samples there is presumably also a net transfer

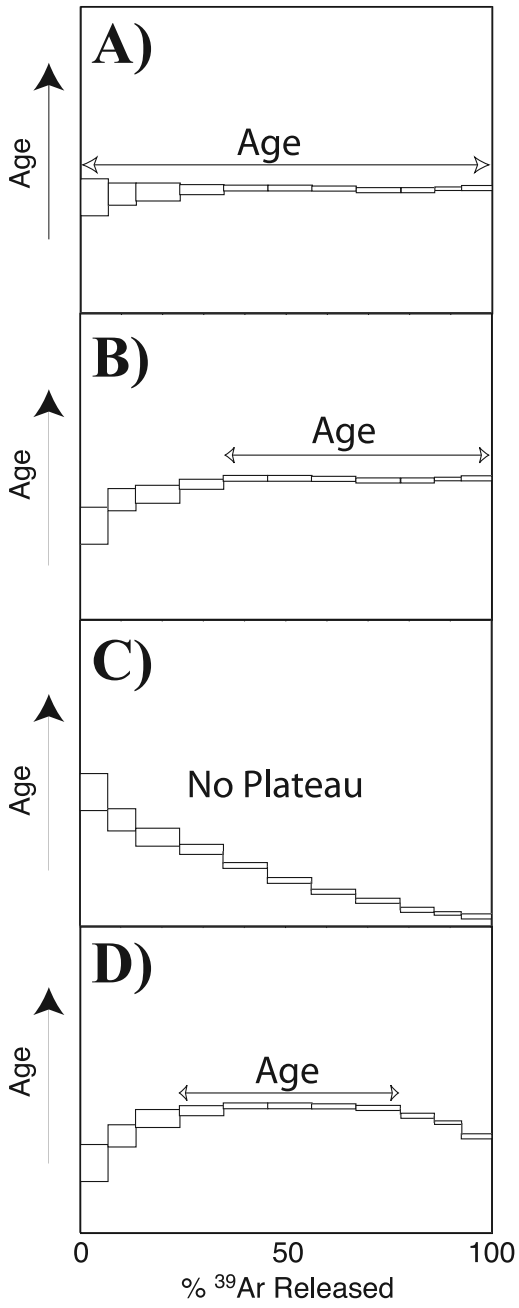

Figure 1. Typical ^{40}Ar-^{39}Ar age spectra for single crystals and expected results in polymineralic, multiage, fine-grained sediment mixtures. (a) Single crystal degassing with homogeneous distribution of argon. In the case of a sediment mixture, a long-plateau age like the one shown would require that all minerals degas synchronously or that all minerals are the same age, which are both unlikely. (b) Argon loss in either single crystals or polymineralic sediment, or the presence of younger, low-temperature minerals. (c) Argon recoil or younger high-temperature minerals (in sediments). (d) Ar loss at low-temperatures and Ar recoil at high temperatures in single crystals or bulk sediment, or younger low-temperature and high-temperature minerals.

of ^{39}Ar from K-rich to K-poor phases, making the K-rich components ''too old'' and the K-poor portions ''too young'' [*Turner and Cadogan*, 1974]. Since K-rich phases outgas at low temperatures and K-poor phases outgas at high temperatures, Ar recoil can usually be recognized by an ever decreasing step age with increasing temperature in the age spectrum (Figure 1c; *McDougall and Harrison* [1999]). Recoil can also transfer ^{37}Ar from Ca-rich to Ca-poor phases, resulting in undercorrection or overcorrection of ^{36}Ar interferences and a similar ''inverse staircase'' effect on the age of the spectrum. Combinations of Ar loss and recoil are also possible (Figure 1d).

[11] In fluvial material, or the terrigenous fraction of marine sediments, it is expected that the age and K/Ca spectra will be different from analyses performed on a single mineral since the bulk sediments are multiage and polymineralic. Age spectra may display variability in step ages and K/Ca throughout the heating schedule. This has been seen before in multiphase samples, where irregular spectra have been obtained from old xenoliths carried in young basalt flows [*Gillespie et al.*, 1982], meteorites showing bimodal trends in their K/Ca spectra due to the temperature-dependent degassing of plagioclase and pyroxene [*Wang et al.*, 1980] and mixtures of detrital K-feldspar grains showing complex degassing patterns [*Copeland et al.*, 1990]. Features like these might be observed in bulk sediment samples. However, previous studies show that concordant steps in polymineralic detritus might also be expected [*Dong et al.*, 1995; *Hemming et al.*, 2002; *Pettke et al.*, 2000].

3. Study Area

[12] Our ultimate goal is to develop methodologies to identify terrigenous sources for deep-sea sediment derived from the Pacific continental margin of northern California, Oregon and Washington. This is part of a larger project relating glacial-interglacial changes in downcore pollen and radiolaria assemblages [*Pisias et al.*, 2001] to terrigenous sediment provenance as a means to distinguish continental vegetation changes from oceanic circulation changes, although the method has broader utility.

[13] To characterize sediments entering this region of the Pacific Ocean for the purpose of tracing sources and transport pathways, we have obtained samples from the mouths of fourteen rivers in the Pacific Northwest (Figure 2). From San Francisco Bay to the Straits of Juan de Fuca, these rivers drain a diverse set of geologic provinces. In Washington, the rocks of the Olympic Mountains are composed of a suite of sandstones, mudstones and volcanic lithologies that have Eocene to Miocene depositional ages [*Brandon and Vance*, 1992]. The Quinalt River sample represents this region (QUI-1). In the southwestern coastal ranges of Washington and northwestern Oregon, rivers erode Eocene sedimentary and volcanic rocks [*Walker and MacLeod*, 1991]. Samples were taken from Grays Harbor (GRA-1), Willapa Bay (WIL-2 and 4), and Tillamook Bay (TIL-1 and 2).

[14] The Columbia River drains an immense area (Figure 2) and a large variety of rock types and geologic provinces with various cooling ages. Lithologies in the headwaters of the Columbia River (including the Kootenay

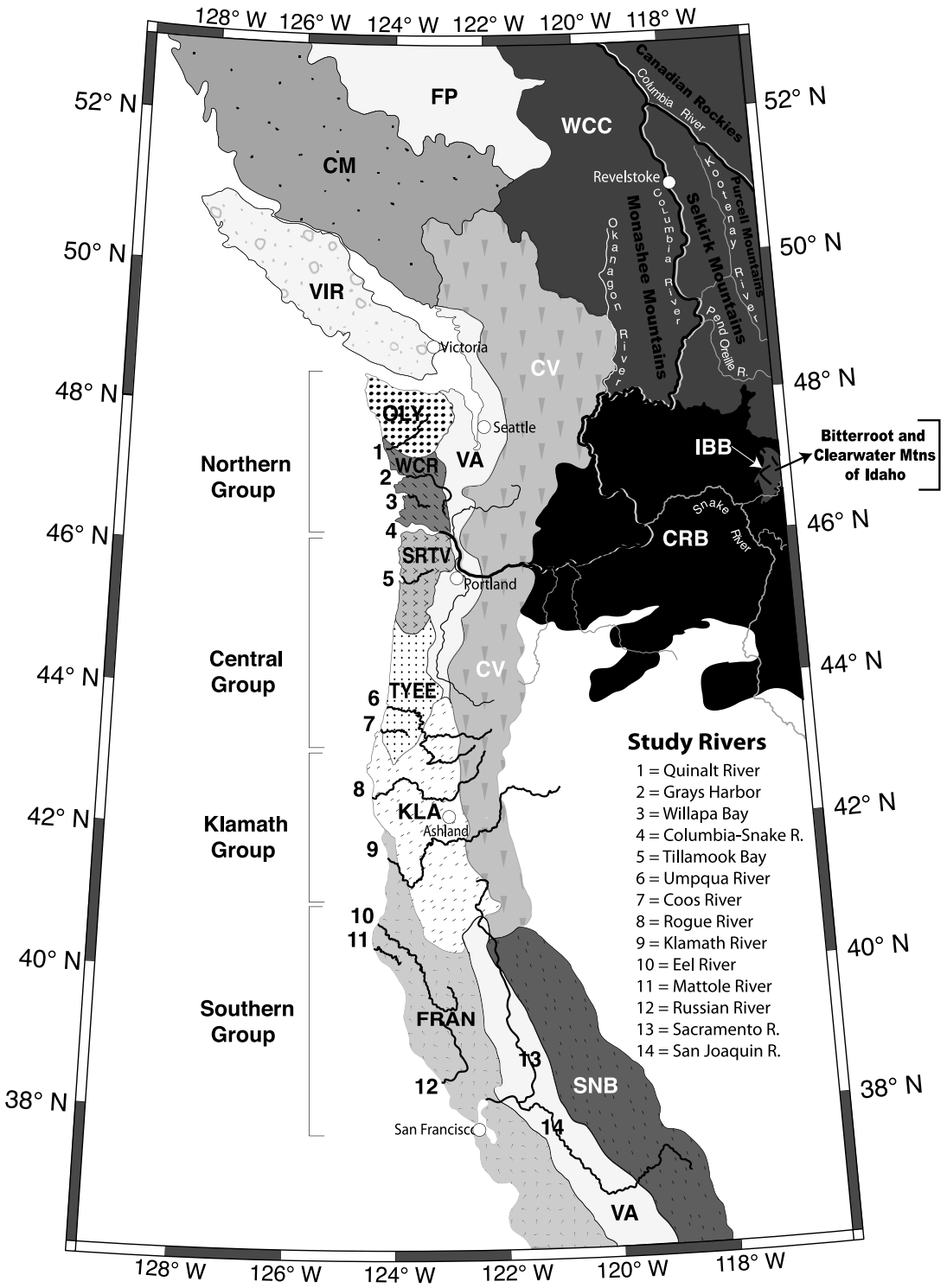

Figure 2. Location map showing study rivers and generalized bedrock geology of the western North America. The geologic provinces shown are those that contribute to the fluvial sediment compositions of the study rivers (except for VIR, CM, and FP). Major Columbia River tributaries and British Columbia mountain belts are shown for reference. The far eastern portion of the Columbia River Basin is not shown for space considerations. OLY, Olympic Mountain Accretionary Complex; WCR, Washington Coast Ranges; SRTV, Siletz River–Tillamook Volcanics; TYEE, Tyee Formation Turbidites; KLA, Klamath Mountain Accretionary Complex; FRAN, Franciscan Melange; VA, Valley Alluvium; SNB, Sierra Nevada Batholith; CV, Cascade Volcanics; CRB, Columbia River Basalts; WWC, Western Canadian Cordillera; IBB, Idaho-Bitterroot Batholith; VIR, CM, and FP, Vancouver Island Ranges, Coast Mountains, and Fraser Plateau (do not contribute to Columbia River). See text for an explanation of lithologies.

and Okanogan River tributaries) in British Columbia are Mesozoic accreted terranes of sedimentary, volcanic and plutonic origins as well as many stocks that intruded into the accreted units [*Ghosh*, 1995; *Monger et al.*, 1982]. The Snake River, a large tributary of the Columbia River, erodes mostly Cretaceous Idaho-Bitterroot Batholith granites in the high-relief regions and then flows across young Tertiary volcanic rocks in the Snake River Plain. The headwaters of the Pend Oreille–Clark Fork and Clearwater tributaries drain the 55–62 Ma granitic batholiths of the Bitterroot Mountains and metasedimentary rocks with Mesozoic to Paleozoic depositional ages from the Rocky Mountains of Montana. Over much of the Columbia Basin, the Columbia River and tributaries erode and flow through the vast area of Miocene Columbia River Basalts and the Tertiary to Recent arc volcanic rocks of the Cascade Mountains. Five samples were analyzed from the Columbia River (COL-1, 3, 5, 1341 and 1498).

[15] Rivers along the central Oregon coast drain turbidite sequences and oceanic basalts with Eocene depositional ages (Coos River, COO-1A and 1C). The Umpqua River (UMP-1A, 1B, and 902) begins in Cenozoic basaltic and andesitic rocks of the central and southern Oregon Cascades and traverses the turbidites of the Oregon Coast Ranges en route to the Pacific Ocean. In southern Oregon and northern California, rocks of the Klamath Mountains are a Mesozoic accretionary complex composed of metasedimentary, metavolcanic, granitic and gabbroic rocks and ophiolitic sequences eroded by the Rogue River (ROG-1A, 4, and 5) and the Klamath River (KLA-1, 2, 4 and 898). Both the Rogue and Klamath Rivers also have significant portions of their headwaters in the volcanic rocks in the southern Cascade Mountains.

[16] The coastal range of northern and central California is dominated by the Franciscan Melange, a Cretaceous to lower Tertiary sequence of sandstones and mudstones, with large blocks (up to several kilometers in size) of serpentinite, blueschist, eclogite greenstone, chert and limestone [*Blake and Jones*, 1981; *McLaughlin et al.*, 1994], although other less extensive volcanic lithologies are present in the region as well. The Eel (EEL-1A, 1B and 2), Mattole (MAT-1) and Russian Rivers (RUS-1 and 2) drain this region. The southernmost rivers (Sacramento and San Joaquin Rivers) drain the granitic rocks of the Mesozoic Sierra Nevada Mountains, Great Valley sediments and lesser contributions from the Klamath and Franciscan rocks. These rivers are represented by SAC-1 (Sacramento River), SAN-1 (San Joaquin River) and SCN-1 (sample from the confluence of the Sacramento and San Joaquin Rivers).

4. Sampling Methods

[17] We sampled from riverbeds either by hand or using a PVC hand sampler in a skiff or by wading. To avoid tidally derived sediment, most samples were taken from riverbeds above the saltwater-freshwater interface. However, some samples were collected in estuaries because this is often where several sediment sources mix before being flushed into the open ocean during storm events. We wanted to capture the most representative samples that enter the ocean, but at the same time, avoid beach material transported into the estuary by tidal processes [*Peterson et al.*, 1984]. In the cases of Willapa Bay and especially Tillamook Bay, attempting to achieve these goals were unsuccessful since it was necessary to collect samples before the point where all main rivers and streams culminate.

[18] Typically, several samples were collected from each river. Most samples were taken in shallow, lower-energy environments where fine-grained material was deposited, such as the downstream side of point bars, sidebars and small embayments. When possible, samples were also taken in mainstream sections. Fine-grained samples were our target since the suspended load that is transported by ocean currents to continental margin sites is of a small particle size. We assume that the fine-grained material sampled here is representative of material that is transported to the ocean but falls out of suspension in the lower-energy point bar, sidebar and embayed environments. All samples were collected during low-flow conditions in the early summer of 2002, except COL-1341 and COL-1498, UMP-902 and KLA-898, which were collected in the mid-1970s (Oregon State University Marine Geologic Core Repository).

5. Analytical Procedures

[19] The 20–63 μm size fraction was extracted from about 100–300 g of bulk material by sieving at 63 μm and then using settling times from the stokes equation to remove the 0–20 μm fraction. The organic compounds were removed by initially adding 30 ml of 35% hydrogen peroxide to the samples. After eight hours of organic oxidation an additional 30 ml of the hydrogen peroxide was added and the samples were shaken for 72 hours. Two hydrogen peroxide steps were needed because of the high organic content in the river sediments. Three washes in distilled water followed. Carbonate was removed by adding 200 ml of dilute acetic acid to each sample and then samples were shaken for 24 hours. The samples were then washed in distilled water three more times. All preparation steps were performed at room temperature.

[20] Irradiation of ~50 mg of sample packaged with the FCT-3 monitor standard (age = 28.03 ± 0.18 Ma; *Renne et al.* [1994]) occurred for six hours in the core of the 1 MW reactor to induce the reaction ^{39}K (n, p) ^{39}Ar. The irradiated samples were analyzed using the MAP 215-50 mass spectrometer in the Ar geochronology laboratory at Oregon State University. Samples were loaded into a Cu sample holder, placed in a vacuum chamber and heated incrementally with a defocused 10W CO_2 laser programmed to traverse the sample during each heating step (for approximately five minutes). Samples were degassed with 13 to 15 temperature steps, from 200° to 300°C to fusion at around 1400°C. Laser temperature was calibrated to laser power with a pyrometer. For each laser-heating step, the extracted gas was exposed to Zr-Al getters for five minutes to remove active gases before measurement in the mass spectrometer. A five-minute pump out time was used between samples. Four blanks were run per sample in order to make corrections throughout sample analysis. Isotopic masses for ^{40}Ar, ^{39}Ar, ^{38}Ar, ^{37}Ar and ^{36}Ar were measured, with the latter three used to correct for interferences on ^{40}Ar and ^{39}Ar [*McDougall and Harrison*, 1999] The most important of these corrections is an atmospheric correction of ^{40}Ar via

Table 1. Common Ranges of K/Ca Values Found in Major K- and Ca-Bearing Minerals in Their Order of Ar Release Temperature (Activation Energy)[a]

Mineral	K/Ca
Kaolinite	4
Vermiculite	0.03
Illite	15
Biotite	10–800
K-Feldspar	10–400
Orthoclase	25–60
Microcline	42
Sanidine	55
Cpx	0–0.04
Opx	0–0.02
Plagioclase	
Albite	0.20–0.52
Andesine	0.10–0.20
Bytownite	0.01–0.10
Anorthite	0.003–0.02
Amphibole	0.06–0.20

[a]Ar release temperature increases down the table. Note that different potassium feldspar and plagioclase members do not necessarily release argon at different temperatures. K/Ca values are from *Deer et al.* [1992], the GEOROC database (http://georoc.mpch-mainz.gwdg.de/georoc/), *Barnes* [1987], and *Barnes et al.* [1986, 1992a, 1992b]. The order of release temperature is based on activation energies from a review paper by *Brady* [1995, and references therein], as well as *Fechtig and Kalbitzer* [1966]. Cpx, clinopyroxene; Opx, orthopyroxene.

the $^{40}Ar/^{36}Ar$ ratio and reactor-induced ^{39}Ar and ^{36}Ar interferences from Ca that are corrected via ^{37}Ar.

[21] The plateau and integrated (total fusion) ages were calculated from corrected $^{40}Ar/^{39}Ar$ ratios using ArArCalc [*Koppers*, 2002]. A variety of corrections were made including those related to mass fractionation and short-lived radioactive decay, while error propagation was applied to every step-heating analysis and correction. Computations of the weighted age plateau and an estimate of its goodness of fit were determined as well. A plateau age, as defined for this study, is any age spectrum that has 50% or more of its total ^{39}Ar characterized by concordant steps [*Koppers*, 2002; *McDougall and Harrison*, 1999]. A mean square of weighted deviations (MSWD) calculation was made for every plateau age to assess the goodness of fit. When this value is much greater than the expected value of one, it suggests that errors on the weighted plateau are underestimated, while a value much less than one suggests that the weighted plateau error is likely to be overestimated [*Koppers*, 2002; *McDougall and Harrison*, 1999; *Wendt and Carl*, 1991].

[22] Potassium-calcium ratios (K/Ca) were also calculated in ArArCalc from measured concentrations of ^{39}Ar derived from K and ^{37}Ar derived from Ca. This ratio was then multiplied by a constant of 0.43 (determined from a monitor standard with a known K/Ca ratio [*Dalrymple et al.*, 1981; *McDougall and Harrison*, 1999]) to arrive at the K/Ca values presented here. A subset of samples (16 of the 33) was analyzed for their K and Ca concentrations, using standard ICP-OES (inductively coupled plasma-optical emission spectrometer) techniques following procedures by *Walczak* [2006]. These were compared with K/Ca values determined from the step-heating Ar analyses and are discussed later in the paper.

[23] The K/Ca values from the step-heating Ar data are also compared with published K/Ca ratios of the major K- and Ca-bearing minerals from the source rocks of geologic provinces in the study area [*Deer et al.*, 1992; GEOROC database, available at http://georoc.mpch-mainz.gwdg.de/georoc/; *Barnes*, 1987; *Barnes et al.*, 1986, 1992a, 1992b] to aid in our interpretation of the minerals contributing to the ^{40}Ar-^{39}Ar age spectra. These K/Ca values for different minerals are presented in Table 1. The minerals are presented in the general order that they most readily diffuse Ar gas as a function of temperature [*Brady*, 1995; *Dalrymple et al.*, 1981; *McDougall and Harrison*, 1999].

[24] Mineralogical identifications by X-ray diffraction (XRD) are presented from eleven Pacific Northwest fluvial samples to underscore our understanding of the gross features dictated by mineralogy in the age and K/Ca spectra. A Scintag Pad-V X-ray diffractometer was used from 5°–64° 2θ using Cu radiation. Samples were sprinkled through a sieve onto slides with double-sided tape and then "razor-tamped" following the procedures outlined by *Zhang et al.* [2003]. This method provides a relatively simple way to attain randomly oriented powders, which are necessary to acquiring quantitative information about mineral abundances. The data were analyzed using MacDiff software (http://www.geologie.uni-frankfurt.de/Staff/Homepages/Petschick/RainerE.html). Relative mineral abundances were calculated on a quartz-free basis.

6. Analytical Results

6.1. ^{40}Ar-^{39}Ar Age Spectra

[25] A summary of results from the 33 ^{40}Ar-^{39}Ar incremental heating experiments is presented in Table 2. Bulk sediment plateau ages for Pacific Northwest river samples range from 76 Ma to 156 Ma. Twenty-two of the 33 samples produced multistep, concordant ages in the middle- to high-temperature portions of their age spectra, accounting for at least 50% of the total gas released from the bulk polymineralic sediment. We term the weighted mean of these concordant step ages a plateau age, remembering that these step ages are the result of congruent degassing of several phases. Because of lower ages in the low-temperature steps (likely from ^{40}Ar loss), the total fusion ages, obtained by summing all gas fractions and comparable to a conventional K-Ar age, are usually younger than the plateau ages, although most samples have a plateau age within 10% of the total fusion age.

[26] The samples are organized into four geographic/lithologic groups (Figure 2): The Northern group (sediments from coastal Washington rivers and the Columbia River), the Central group (sediments from coastal Oregon rivers south of the Columbia River to ~43°N latitude), the Klamath group (sediments from the Rogue and Klamath Rivers eroding the Klamath Accretionary Complex), and the Southern group (northern and central Californian river sediments).

[27] The plateau ages for the Washington coastal river sediments range from 121 to 125 Ma (Figure 3). The QUI-1 (Quinalt River) age spectrum does not develop a plateau. Step ages increase until a short, three-step maximum of 157 Ma. GRA-2, which was taken from the confluence of the Chehalis and Hoquiam Rivers in Grays Harbor, shows an initial ramp up in step ages followed by a five-step plateau (50% of the total gas) at 121 Ma and finishes with

Table 2. Summary of ^{40}Ar-^{39}Ar Incremental Heating Experiments for Pacific Northwest River Sediments[a]

Sample Name	Latitude, °N	Longitude, °W	Total Fusion, Ma	Plateau Age, Ma	2σ Error	Steps	Percent ^{39}Ar	MSWD	Plateau K/Ca	Integrated K/Ca
				Northern						
QUI-1	47.35	124.29	103.8	156.6	2.5	3	19.8	1.5	0.14	0.33
GRA-2	46.97	123.80	114.3	121.1	1.2	5	50.3	0.5	0.42	0.30
WIL-2	46.72	123.93	112.3	no plateau	NA	NA	NA	NA	NA	0.53
WIL-4	46.72	123.93	115.4	124.8	2.2	6	64.3	14.0	0.36	0.26
COL-1 LP	46.25	123.36	108.3	103.0	1.0	5	48.9	1.0	0.38	0.30
COL-1 HP				113.3	1.4	3	26.0	0.4	0.28	
COL-3 LP	46.25	123.49	111.7	108.9	1.3	4	48.9	0.8	0.32	0.25
COL-3 HP				124.7	3.9	3	21.2	9.5	0.29	
COL-5 LP	46.24	123.62	123.8	112.5	4.6	3	33.3	10.4	0.35	0.28
COL-5 HP				138.1	1.5	4	33.8	0.6	0.38	
COL-1341 LP	[b]	[b]	125.7	106.1	1.4	7	27.6	1.4	0.69	0.54
COL-1341 HP				133.8	1.3	6	47.9	1.8	0.48	
COL-1498	[b]	[b]	72.2	141.0	2.3	3	8.4	0.2	0.52	0.79
				Central						
TIL-1	45.48	123.90	102.6	110.5	1.2	8	73.6	3.0	0.26	0.41
TIL-2	45.48	123.90	73.1	76.5	0.8	6	57.0	1.1	0.15	0.11
UMP-902	[b]	[b]	93.6	100.3	0.9	8	54.0	0.2	0.44	0.50
UMP-1A	43.70	124.07	84.0	88.3	0.6	8	79.2	1.1	0.52	0.66
UMP-1B	43.70	124.07	85.4	88.5	0.9	8	75.5	1.3	0.10	0.14
COO-1A	43.38	124.18	92.5	99.9	0.5	3	41.2	0.8	0.47	0.33
COO-1C	43.38	124.18	87.9	94.2	1.8	6	58.6	12.7	1.71	1.75
				Klamath						
ROG-900	[b]	[b]	116.7	124.9	1.5	11	71.0	2.0	0.21	0.34
ROG-1A	42.44	124.40	128.0	131.7	0.9	10	88.6	2.2	0.14	0.32
ROG-4	42.44	124.38	117.9	127.2	2.0	9	79.8	1.7	0.12	0.17
ROG-5	42.44	124.38	124.0	130.5	1.5	7	71.2	0.5	0.19	0.30
KLA-898	[b]	[b]	144.3	156.0	1.4	7	44.4	2.1	0.30	0.44
KLA-1	41.52	124.00	126.9	no plateau	NA	NA	NA	NA	NA	0.33
KLA-2	41.52	124.02	137.2	148.1	1.6	6	51.6	2.1	0.14	0.25
KLA-4	41.23	123.65	141.3	149.5	1.9	8	80.6	2.4	0.14	0.15
				Southern						
EEL-1A	40.64	124.28	124.6	131.7	0.8	5	65.5	1.6	0.90	0.95
EEL-1B	40.64	124.28	123.3	126.6	1.5	8	84.3	2.1	0.69	1.07
EEL-2	40.63	124.28	122.4	128.7	1.0	6	64.9	1.1	1.09	1.12
MAT-1	40.31	124.28	67.3	77.9	1.8	5	46.2	3.4	0.69	0.66
RUS-1	38.43	123.10	106.7	110.9	0.9	10	83.3	1.4	0.33	0.76
RUS-2	38.43	123.10	108.5	116.3	1.2	6	68.1	1.1	0.27	0.19
SCN-1	38.07	121.86	118.2	123.7	1.0	7	62.8	0.6	0.28	0.43
SAC-1	38.06	121.79	121.7	125.6	1.5	5	67.7	2.6	0.47	0.56
SAN-1	38.03	121.86	119.1	120.4	0.9	11	95.6	1.2	0.39	0.48

[a]Steps, the number of steps that characterize the plateau; MSWD, mean square of weighted deviations [*Koppers*, 2002]. LP, low-temperature plateau; HP, high-temperature plateau.

[b]No precise location information is available for COL-1341, COL-1498, UMP-902, ROG-900, or KLA-898 (collected at the mouths of these rivers by J. Dymond and G. R. Heath).

increasing step ages until fusion. For Willapa Bay, WIL-2 shows a continuous increase in age throughout the age spectrum while WIL-4 developed a six-step plateau containing 64% of the gas, at 125 Ma. Four out of five Columbia River samples display two fairly distinct plateaus in their age spectra (Figure 3). The lower-temperature plateaus range from 103 to 113 Ma while the higher-temperature plateaus range between 113 and 138 Ma. These are the only samples from our study that show this dual plateau pattern. All samples in the northern group show evidence for minor Ar loss. We observe that most of these age spectra increase in age at the highest-temperature steps, suggesting that no significant Ar recoil has occurred and that older, high-temperature minerals are present (amphiboles?).

[28] River sediments from Oregon coastal rivers in the Central group are, as a whole, the youngest in the data set (Figure 4). The age spectra for the seven samples show an initial increase in the step ages with temperature, followed by broad, multistep plateaus that either continue to fusion or are followed by a slight decrease in step age, likely related to Ar recoil. The two samples from Tillamook Bay show good plateaus, but two markedly different ages (76.5 and 110.5 Ma). UMP-1A and 1B are identical in age (88.3 and 88.5 Ma, respectively), while UMP-902 (precise sampling location within the river is uncertain) is significantly older at 100 Ma. The Coos River sediment age spectra show similar patterns, with middle-temperature plateaus (94–100 Ma) and decreasing step ages at higher temperatures, indicative of Ar recoil.

[29] The Rogue River and Klamath River sediments (Klamath group) show consistent within-river results, but differ notably in between-river bulk sediment ages and degassing patterns (Figure 5), even though both rivers erode

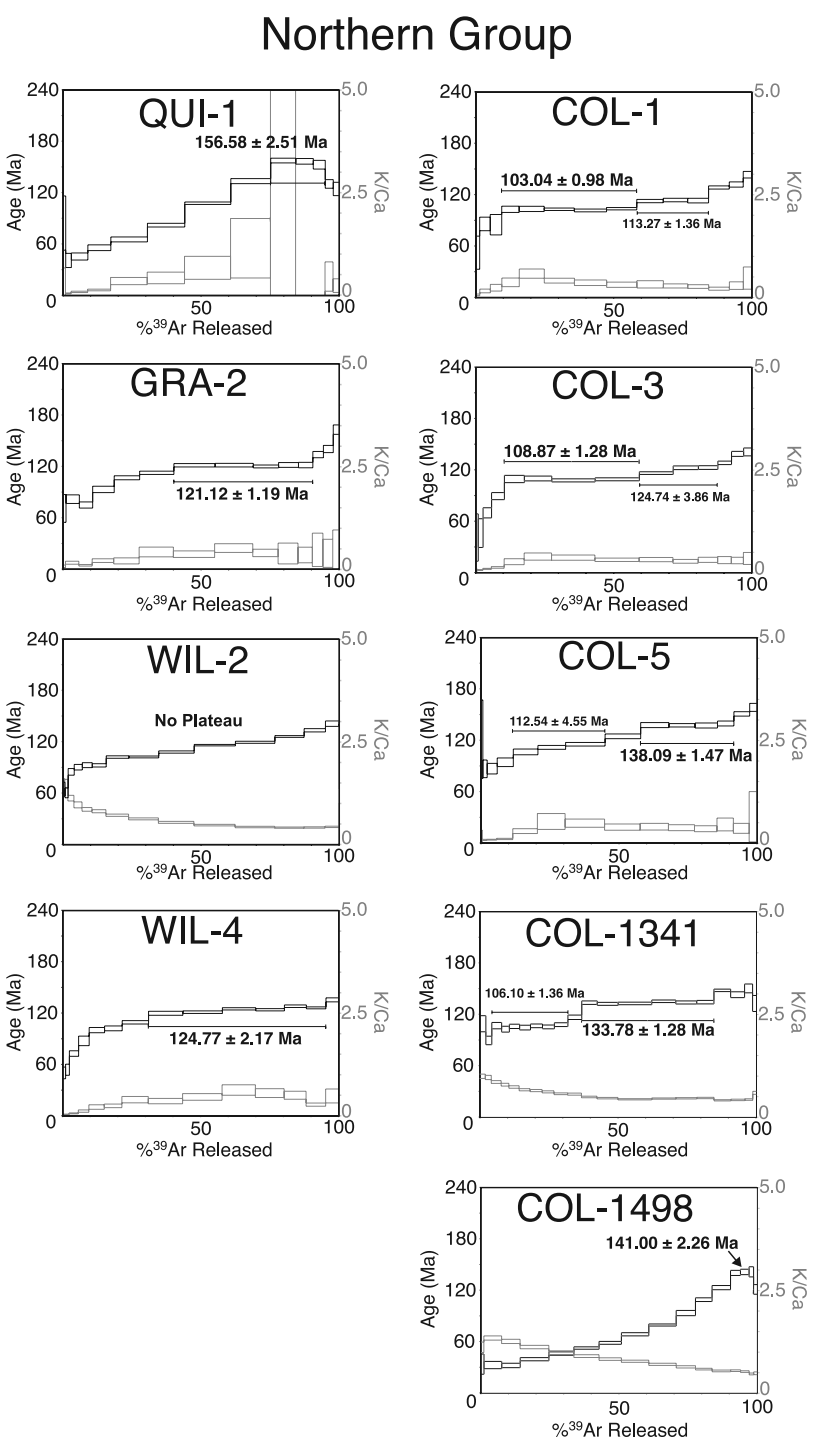

Figure 3. ^{40}Ar-^{39}Ar incremental heating spectra and K/Ca spectra for river sediments from the Northern group (coastal Washington and Columbia watersheds) of the Pacific Northwest. Age spectra are black while the K/Ca spectra are gray. Analytical uncertainties (2σ) related to age and K/Ca are depicted by the vertical scaling of each step-heating box.

the same rocks in the Klamath Mountains. All four of the Rogue River samples produced good plateaus whose ages fall between 125 and 132 Ma. Their degassing patterns are very similar as well, with little evidence for recoil effects in the high-temperature steps. Three of the four Klamath River samples show similar ages, between 148 and 156 Ma. The degassing pattern is somewhat different from the Rogue River samples, increasing in age over a greater temperature range initially, with a clear but narrower plateau. One sample (KLA-1) did not develop a plateau. It appears to contain a small proportion of some significantly older mineral that outgassed at high temperatures. Generally, the samples in the Klamath group show no consistent recoil patterns.

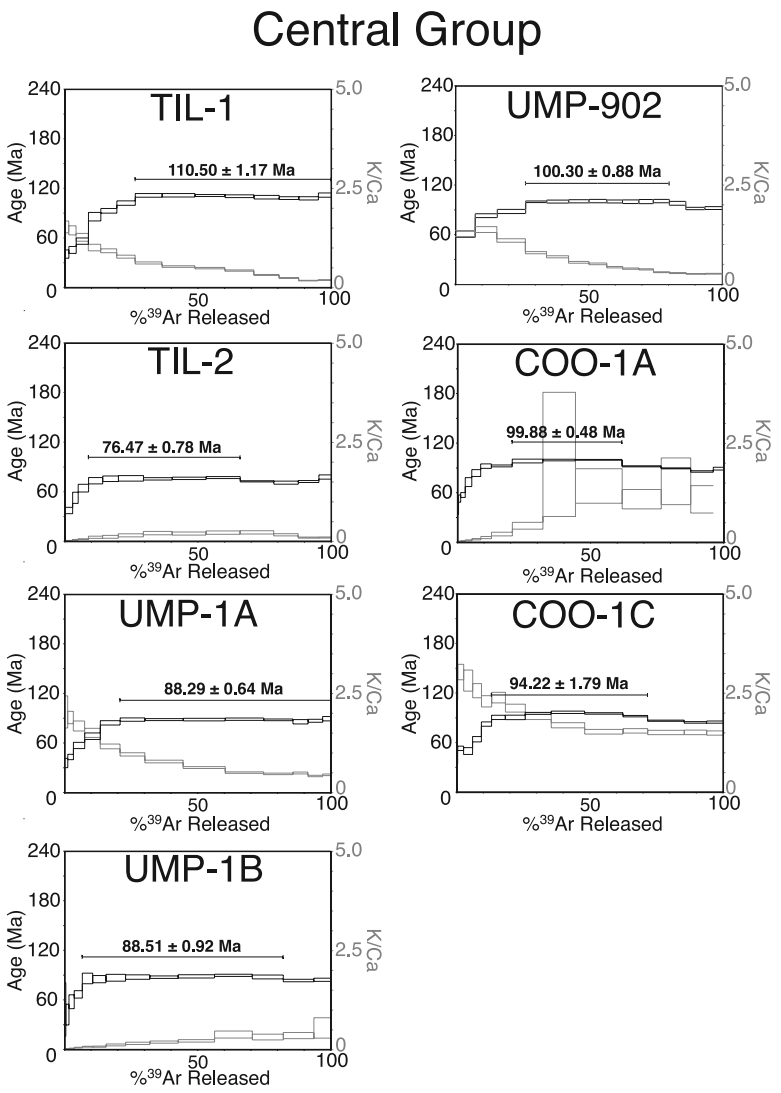

Figure 4. ^{40}Ar-^{39}Ar incremental heating spectra and K/Ca spectra for river sediments from the Central group (coastal Oregon) of the Pacific Northwest. Age spectra are black while the K/Ca spectra are gray. Analytical uncertainties (2σ) in age and K/Ca are depicted by the vertical scaling of each step-heating box.

[30] The Eel, Mattole, Russian, Sacramento and San Joaquin Rivers comprise the Southern group (Figure 6). The three samples from the Eel River are quite similar in age (127–132 Ma) and degassing pattern, with broad plateaus and decreasing step ages at the highest temperatures. MAT-1 is one of the youngest samples in the data set (78 Ma), with five concordant steps comprising just under 50% of the total gas released, and is much younger than the geographically adjacent Eel River samples. It drains a relatively small Miocene-Cretaceous sedimentary subunit of the Franciscan Melange Coastal Belt [*McLaughlin et al.*, 1994] not shown in Figure 2. The spectra of the two Russian River samples produced good plateaus at 111 and 116 Ma. Although the ages differ somewhat, the Russian River samples share many of the features seen in the Eel River samples (Figure 6). Samples from both yield increasing step ages (30–60 Ma) for three to five steps then arrive at a plateau throughout the middle-temperature steps and terminate with decreasing ages for the highest-temperature steps. Both the Eel and Russian Rivers erode the Franciscan Melange, but a significant portion of the Russian River also erodes the Miocene-Pliocene Sonoma and Tolay volcanic rocks [*Fox et al.*, 1985], which may explain the small age difference between the two rivers. The three southernmost samples from the Sacramento and San Joaquin Rivers have an average plateau age of 123 Ma. These samples display broad, continuous plateaus throughout the stepwise heating process, after only a short low-temperature set of steps affected by ^{40}Ar loss. Ar recoil appears to be important in the Eel, Mattole and Russian Rivers over the highest-temperature steps, but not in the Sacramento–San Joaquin samples.

6.2. Mineralogy and K/Ca Spectra

[31] XRD analyses performed on a subset of samples showed that, in order of relative abundance, the most abundant mineral is plagioclase (Table 3), followed by clinopyroxene, kaolinite, K-feldspar, vermiculite, horn-

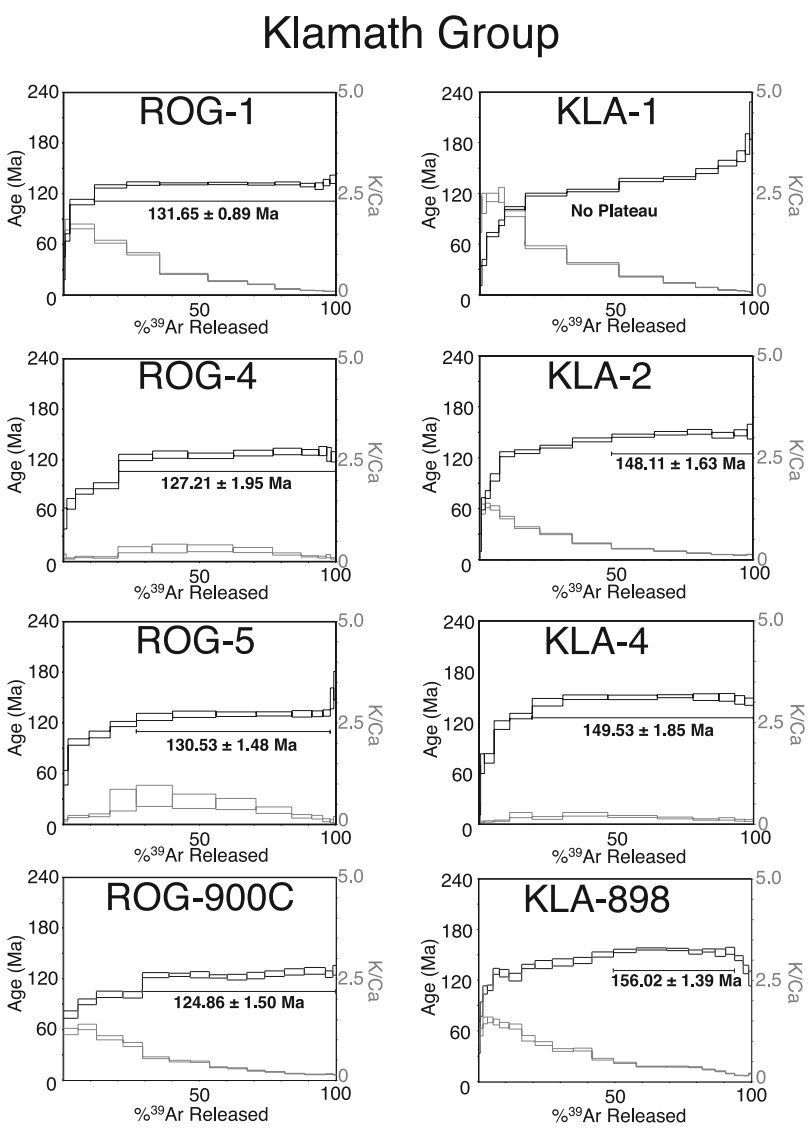

Figure 5. ^{40}Ar-^{39}Ar incremental heating spectra and K/Ca spectra for river sediments from the Klamath group (southern Oregon and northern California) of the Pacific Northwest. Analytical uncertainties (2σ) in age and K/Ca are depicted by the vertical scaling of each step-heating box.

blende (amphiboles), orthopyroxene and biotite (and other micas). Minerals releasing gas at the lowest temperatures are clays such as kaolinite and vermiculite. Their K/Ca ratios (Table 1; *Deer et al.* [1992]) are low to moderate at 0.03–4.0. Although clays, strictly speaking, do not exist in the 20–63 μm fraction, they are present in our samples presumably by adhesion to larger grains. Biotite, muscovite, illite and other micas have high K/Ca values (K/Ca = 10–800 [*Deer et al.*, 1992; GEOROC database, available at http://georoc.mpch-mainz.gwdg.de/georoc/; *Barnes*, 1987; *Barnes et al.*, 1986, 1992a, 1992b]). The micas release gas at moderate temperatures [*Brady*, 1995; *Dalrymple et al.*, 1981; *McDougall and Harrison*, 1999], suggesting that the K/Ca ratios in bulk sediments during the low-temperature to midtemperature steps are likely to be influenced by these minerals, even though they are not overly abundant in the samples. Orthoclase, microcline and sanidine of the K-feldspar group degas at low (microcline and sanidine) to moderate (orthoclase) temperatures, with K/Ca ratios that are high (K/Ca = 10–400 [*Deer et al.*, 1992; GEOROC database, available at http://georoc.mpch-mainz.gwdg.de/georoc/; *Barnes*, 1987; *Barnes et al.*, 1986, 1992a, 1992b]). These minerals should produce obvious signatures in the K/Ca spectra, even if present in only low abundances. Pyroxenes degas at moderate to high temperatures and, although not a significant carrier of K, they have relatively high Ca concentrations (and correspondingly low K/Ca values between 0 and 0.04). Plagioclase and hornblende have low K/Ca ratios, ranging from 0 to 0.5 (Table 1). Although amphiboles are the most retentive [*Brady*, 1995; *Dalrymple and Lanphere*, 1969], they are found in only small amounts. Thus plagioclase is the most likely mineral to be contributing to the age and K/Ca spectra at higher temperatures.

[32] In the Northern group, K/Ca values show a variety of trends in the stepwise heating results. GRA-2, WIL-4, COL-1, 3 and 5 all share similar trends and low values of K/Ca ratios (Figure 3 and Table 2). After an initial rise

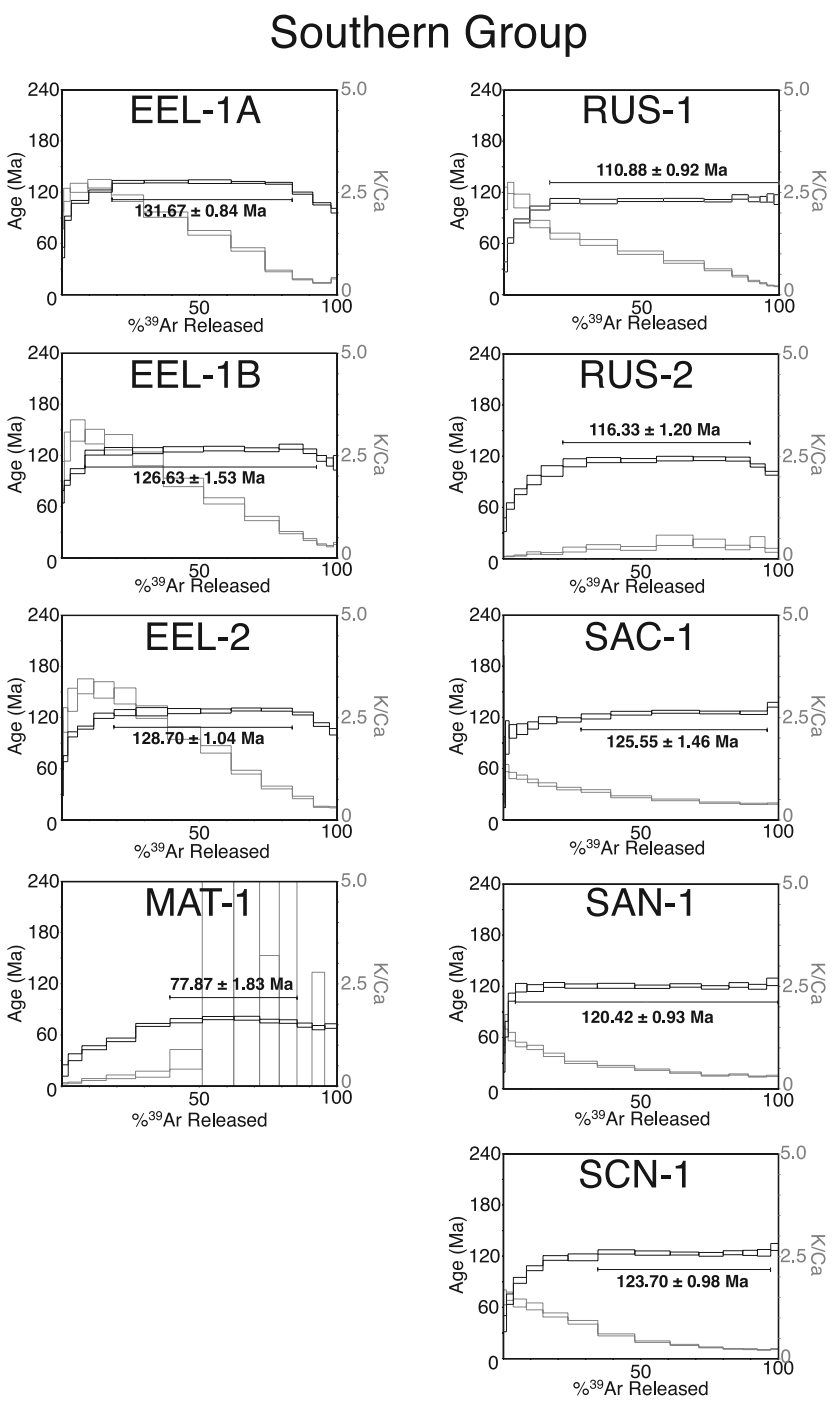

Figure 6. ^{40}Ar-^{39}Ar incremental heating spectra and K/Ca spectra for river sediments from the Southern group (northern and central California). Age spectra are black while the K/Ca spectra are gray. Analytical uncertainties (2σ) in age and K/Ca are depicted by the vertical scaling of each step-heating box.

during the low-temperature heating steps, the K/Ca ratios become uniform at approximately 0.3–0.4, possibly indicative of either a high-K plagioclase or a mixture of a low- or moderate-K plagioclase with a higher-K mineral such as K-feldspar. There is no statistically significant difference in the K/Ca values over the two plateau intervals observed in the Columbia River age spectra.

[33] Potassium-calcium trends in the Central group are also variable (Figure 4 and Table 2). The Tillamook Bay samples show different trends and average values, not surprising considering the age differences. Although the ages for UMP-1A and 1B are virtually identical, their respective K/Ca trends are quite different in the low-temperature steps. UMP-1A begins at about K/Ca = 2.4 and decreases continually until the latter stages of the step-heating process, where K/Ca ratios trend toward a uniform value of about 0.5. UMP-1B, on the other hand, increases from very low K/Ca values to an average of about 0.1 that sustains until fusion. UMP-1A may have more high-K minerals degassing in the low-temperature steps (such as

Table 3. Mineralogic Abundances for Major K- and Ca-Bearing Minerals as Determined From X-Ray Diffraction of 11 Samples[a]

Sample	Latitude, °N	Plagioclase	Cpx	Kaolinite	Orthoclase	Vermiculite	Hornblende Amphibole	Opx	Biotite Mica
QUI-1	47.4	61	15	7	8	3	1	3	2
COL-3	46.3	68	8	1	9	3	2	7	2
COL-5	46.2	67	13	1	10	1	2	4	1
TIL-4	45.5	45	27	1	9	15	0	4	0
UMP-1B	43.7	55	19	6	11	3	2	3	0
ROG-5	42.4	29	10	21	6	21	8	0	4
KLA-1	41.5	47	15	9	7	3	12	5	2
KLA-4	41.2	27	7	25	5	11	11	5	8
EEL-1A	40.6	43	8	15	8	13	2	6	5
RUS-2	38.4	47	14	10	9	7	4	5	5
SAN-1	38.0	62	16	5	10	1	2	3	2
Average		50	14	9	8	7	4	4	3
Standard deviation (1σ)		14	6	8	2	7	4	2	3
K/Ca model best fit		60	8	4	10	7	4	2	6

[a]Mineralogic abundances are given in relative percent (calculated on a quartz-free basis). The best fit mineralogic abundances used later in the K/Ca degassing model are also shown. TIL-4 is the only sample analyzed by X-ray diffraction from Tillamook Bay and was not characterized by ^{40}Ar-^{39}Ar methods. Cpx, clinopyroxene; Opx, orthopyroxene.

kaolinite and other clays and/or mica), explaining some of the contrast between the two samples. At high temperatures, the K/Ca values are indicative of plagioclase, amphibole and possibly, a small contribution from K-feldspar. The Coos River samples show markedly different K/Ca trends and values despite the fact that their age spectra are quite similar throughout the heating process. COO-1A begins with a very low K/Ca ratio and then steps upward to about 0.5, whereas COO-1C begins at K/Ca $\sim$ 3 and decreases to about 1.7, high values relative to the rest of the data set. The mineralogy comprising the Coos River bulk sediment plateaus must have greater abundances of high-K minerals (such as K-feldspar) than other samples or, conversely, low abundances of high-Ca minerals such as clinopyroxene.

[34] The Klamath group, which is composed of the Rogue and Klamath Rivers, shows rather similar K/Ca trends. Five of the eight samples (ROG-1, ROG-900, KLA-1, 2, and 898) show a continuous decrease in K/Ca ratios during the heating process from K/Ca values of 1.5 (a possible mixture of kaolinite and vermiculite) down to values consistent with a plagioclase characterized by low to moderate K at around 0.1 (Figure 5). The other three Klamath group samples (ROG-4, 5 and KLA-4) show an initial small increase in K/Ca, followed by a short duration of successive steps releasing similar K/Ca values. The final termination is punctuated by small decreases in the K/Ca ratio. The notably low K/Ca values for all samples in the middle- to high-temperature steps suggest a mixture of plagioclase, hornblende and possibly pyroxene.

[35] Trends of K/Ca for the Southern group are generally similar within each river basin. The Eel River samples display relatively high K/Ca ($\sim$2.5) during the low-temperature steps, decreasing steadily to values around 0.3 (Figure 6), consistent with a mineralogy dominated by clays such as kaolinite, mica and possibly a low-temperature K-feldspar (microcline) at the lower temperatures and plagioclase during the middle to high temperatures. The Mattole River sample K/Ca ratios have large analytical uncertainties, suggesting that measurement error on ^{37}Ar (from Ca) was significant. The two Russian River samples have contrasting K/Ca trends. The RUS-1 K/Ca spectra, showing a pattern not unlike the Eel samples, has a high K/Ca contribution (K/Ca $\sim$ 2.5) at the lower-temperature steps, likely from kaolinite and mica while at higher temperatures the lower K/Ca values suggest a mixture of high- and low-K minerals. The consistently low K/Ca values in RUS-2 (K/Ca = 0.2) suggest a K/Ca spectra dominated by plagioclase. All three of the Sacramento–San Joaquin samples display K/Ca patterns that decrease throughout much of the heating experiment. Toward the higher-temperature steps, however, a plateau in the K/Ca ratio centered at 0.3 develops, consistent with plagioclase degassing, and possibly a small contribution of a high-K mineral such as K-feldspar.

[36] In summary, the majority of samples for the entire data set appear to have K/Ca values that are consistent with mostly plagioclase degassing during the middle- to high-temperature steps. This is also the temperature range that tends to develop ^{40}Ar-^{39}Ar age plateaus. However, the K/Ca ratios measured over age plateau–determining steps (K/Ca $\sim$ 0.3) are a bit higher than measurements made on many plagioclases from the Columbia River Basalts, Cascades and Klamath Mountains [*Barnes*, 1987; *Barnes et al.*, 1986, 1992a, 1992b; GEOROC database, available at http://georoc.mpch-mainz.gwdg.de/georoc/] suggesting that a higher-K mineral such as K-feldspar could also be releasing a small amount of Ar during the higher-temperature steps.

7. Evaluating the K/Ca Spectra and Bulk Sediment Ages

7.1. K/Ca Degassing Spectra Reveal Bulk Mineralogy

[37] To help support the connections we have proposed between K/Ca values and mineralogy, we have developed a forward model that predicts K/Ca spectra. The best fitting values from the average abundances for each K- and Ca-bearing mineral (from XRD of 11 samples; Table 3) are used in conjunction with K and Ca concentrations (Table 4). The release of ^{39}Ar and ^{37}Ar (proxies for K and Ca, respectively, described in the analytical section) from each mineral with increasing temperature is assumed to follow a Gaussian distribution.

[38] Each Gaussian degassing curve mean (temperature at which a given mineral reaches a diffusion maximum) and standard deviation (an estimate of the range over which a given mineral diffuses gas) are estimated from the available

Table 4. Range of K and Ca Concentrations Determined From *Deer et al.* [1992], GEOROC Database, *Barnes* [1987], and *Barnes et al.* [1986, 1992a, 1992b][a]

Mineral	K Range, ppm	K/Ca Model Best Fit	Ca Range, ppm	K/Ca Model Best Fit
Kaolinite	1750	1750	425	425
Vermiculite	200	200	12,000	12,000
Mica	60,000–80,000	80,000	100–1000	100
K-spar	100,000–125,000	150,000	600–2000	600
Clinopyroxene	100–300	300	100,000–130,000	100,000
Orthopyroxene	100–300	300	10,000–20,000	10,000
Plagioclase	2000–12,500	12,500	40,000–75,000	40,000
Amphibole	5000–10,000	10,000	60,000–90,000	60,000

[a]The GEOROC database is available at http://georoc.mpch-mainz.gwdg.de/georoc/. K-spar, potassium feldspar.

diffusion data for silicates [*Brady*, 1995; *Fechtig and Kalbitzer*, 1966; *Harrison et al.*, 1985; *Lovera et al.*, 1997; *McDougall and Harrison*, 1999] and correspond with the order of release temperatures presented in Table 1. These degassing patterns are presented in Figures 7 and 8. Little is known about the precise release trends in minerals as a function of temperature [see *McDougall and Harrison*, 1999], so we use the relative relationships about diffusion among minerals expressed through values of activation energy and/or diffusion coefficients [*Fechtig and Kalbitzer*, 1966; *Harrison et al.*, 1985; *Lovera et al.*, 1997; *McDougall and Harrison*, 1999]. The model provides a first-order view of how the various minerals in a polymineralic sample might combine to produce observed K/Ca spectra, acknowledging that the order that these minerals release their gas could be different from what we have chosen, especially with feldspars [*McDougall and Harrison*, 1999].

7.2. K/Ca Model Results

[39] The results of the K/Ca degassing spectra model weighted by (1) the mineral abundances for eight minerals and (2) the amount of K and Ca released at each of seven temperature steps from 200°C to 1400°C are presented in Figure 9. The best fitting model result is plotted along with the average and standard deviation (1σ) of the measured K/Ca values for each temperature step from 24 samples that have not experienced appreciable ^{39}Ar loss.

[40] The modeled K/Ca values are generally in good agreement with the measured values considering the simplifications we have made for the diffusion of gases from these silicate minerals. These results suggest that to a first order, the K/Ca ratios at a given step are simply the average of contributions from the degassing minerals. Although this is intuitive, it is important to show that this simple calculation provides expected K/Ca similar to measured values from the bulk sediment ^{40}Ar-^{39}Ar incremental heating experiments. Moreover, we note that plagioclase, because of its high abundance in the samples and high-temperature range of gas release, is the dominant mineral contributing to the age spectra at middle to high temperatures and therefore is the dominant mineral driving plateau development in these bulk sediment samples.

7.3. Modeling the ^{40}Ar-^{39}Ar Ages of Detrital Mixtures

[41] The observation of reproducible, well-defined plateau ages in the majority of our river samples is an important, yet surprising result considering that the sediment analyzed is a mixture of a variety of detrital minerals. The gas measured during any given temperature step is a mixture of all the contributions from K-bearing minerals releasing Ar at that temperature. To develop well-defined multistep age plateaus, the ages of the suite of minerals degassing from one temperature to the next has to be, in total, the same. For this to occur either an unusually favorable mixture of minerals have to be present where only one or two minerals dominate the gas released during incremental heating, or conversely, all minerals are derived from the same-aged geologic province(s). From the previous discussion we conclude that, since degassing of plagioclase generally coincides with the development of age plateaus and plagioclase abundances are the highest of the major K-bearing minerals, plagioclase dominates the age plateau results. To a lesser extent, K-feldspar could be a factor in some of the age plateaus since it can have an unpredictable degassing pattern over a broad temperature range [*Brady*, 1995; *McDougall and Harrison*, 1999] and has such high K content.

[42] We now take advantage of the finding that plagioclase and K-feldspar are the important minerals dictating release of Ar and develop a simple model to evaluate the meaning of the age spectra. The calculation takes into account mineral K content, cooling age and the proportional

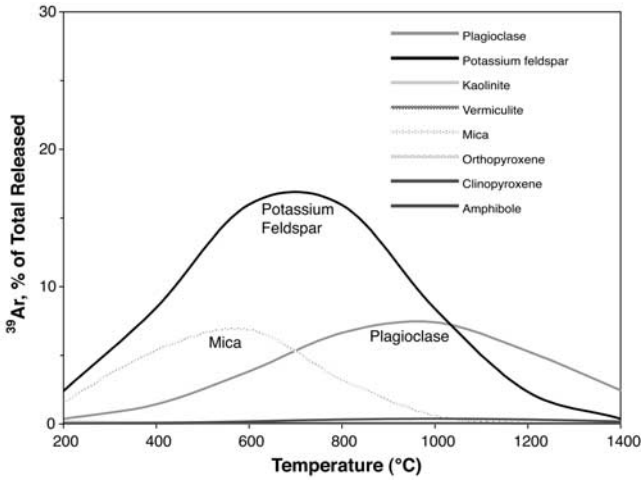

Figure 7. Modeled ^{39}Ar (K) degassing patterns for selected minerals based on published K concentrations (see text and Table 4) and activation energies. Release is expressed as percent of total of all minerals degassing Ar. K concentrations are based on best fit (Table 4). K-feldspar and mica dominate in the low to middle temperatures while plagioclase becomes important at high temperatures.

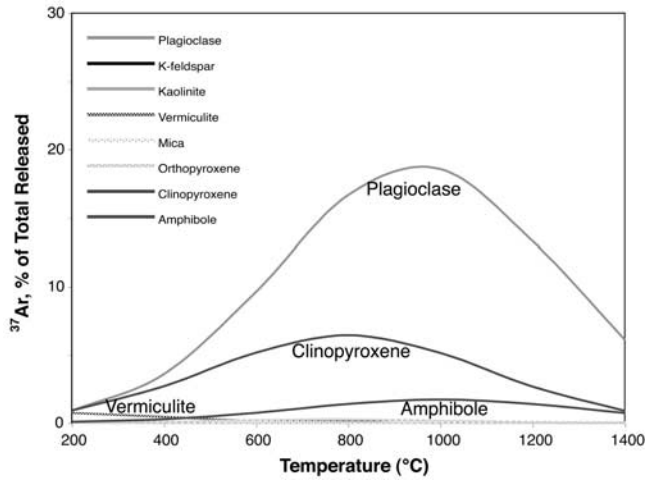

Figure 8. Modeled ^{37}Ar (Ca) degassing patterns for selected minerals based on published Ca concentrations (see text and Table 4) and activation energies. Release is expressed as percent of total of all minerals degassing Ar. Ca concentrations are based on best fit (Table 4). Plagioclase dominates almost the entire release pattern, while clinopyroxene, an insignificant contributor to the age spectra (low K), plays a significant role in the K/Ca spectra.

area of each bedrock unit. We develop the model for the Umpqua, Rogue and Klamath River basins, given the availability of cooling age information and digital geologic maps, which makes calculations of the areas of individual mapped lithologies relatively easy and accurate. The conditions and assumptions are as follows.

[43] On the basis of our age and K/Ca results, we assume that the plateau ages are dominated by K from plagioclase mostly and to a lesser extent, K-feldspar (in which the K concentration for this plagioclase–K-feldspar mixture is weighted by a 95–5% mineral abundance mixture since only a ''tail'' of K-feldspar is likely to be outgassing Ar at the higher, plateau-defining temperatures). Each of the mapped units is assigned K concentrations that are either based on plagioclase only (in the case of mafic or intermediate Cascade rocks as well as sediments derived from basaltic or andesitic compositions) or a mixture of plagioclase and K-feldspar (in the case of granitic units and sediments derived from felsic protoliths). Plagioclase K concentrations differ in the model depending on whether the host rock is felsic (6000 ppm), intermediate (or andesitic; 4000 ppm), mafic (2000 ppm) or ultramafic (1000 ppm). Mixtures of these four values are also used when appropriate.

[44] In the Umpqua River basin, the sedimentary Tyee Formation is divided into two groups derived from different protoliths [*Ryu and Niem*, 1999; *Walker and MacLeod*, 1991]. One half of the Tyee Formation is sourced from the paleo-Klamath Mountains, while the other half is derived from the Idaho Batholith. The Idaho Batholith–derived component is assigned an age of 67 Ma [*Heller et al.*, 1985, 1992] and the Klamath Mountain component is assigned an age of 154 Ma, the average age for all of the Klamath Accretionary Complex plutonic rocks [*Irwin and Wooden*, 1999]. This age is also assigned to metasedimentary terranes in the Klamath Mountains, where we assume an age equivalent to the age of the youngest plutons intruded into them [*Wells et al.*, 2000]. This is feasible since it is likely that most of the K-bearing minerals in these metasedimentary units were reset during contact and regional metamorphism. This allows us to calculate an average age of the Klamath-derived component of the Tyee Formation, which is estimated from the average age of 154 Ma for all plutons with radiometric ages available. For the Cascade arc–derived lithologies, the eleven most common mapped units exposed in the Umpqua River basin were simplified into three age/lithologic groups (Figure 10; *Walker and MacLeod* [1991]). For the age of Cascade rocks in the Rogue and Klamath Rivers a weighted average of 21 Ma (calculated from the 11 units used in the Umpqua Basin) was used, recognizing that this number could realistically range from around 10–30 Ma.

[45] The geologic map of *Irwin and Wooden* [1999] was used for extracting rock type and cooling age parameters in the Rogue and Klamath River basins. The areas of these units were calculated from digital geologic maps of the Klamath Mountains [*Irwin*, 1997]. Most mapped units from *Irwin and Wooden* [1999] smaller than ~50 km^2 were not included in the analysis. Because of this, the summed rock-type areas of all units used in the model do not likely equal the true river basin areas of either the Rogue or the Klamath Rivers. The total area not captured by this simplification is less than 10%.

[46] Finally, this model assumes that erosion occurs evenly over all rock types and in all parts of the basin. Neither are true [*Howard*, 1998; *Howard et al.*, 1994; *Montgomery*, 1994; *Whipple et al.*, 1999; *Whipple and Tucker*, 1999], but at least in the cases provided by the Umpqua and Rogue Rivers, these factors could be negligible, as will be shown in the results. However, differential erosion and/or sediment transport and storage are needed to explain differences between the Klamath River model and ^{40}Ar-^{39}Ar plateau age results.

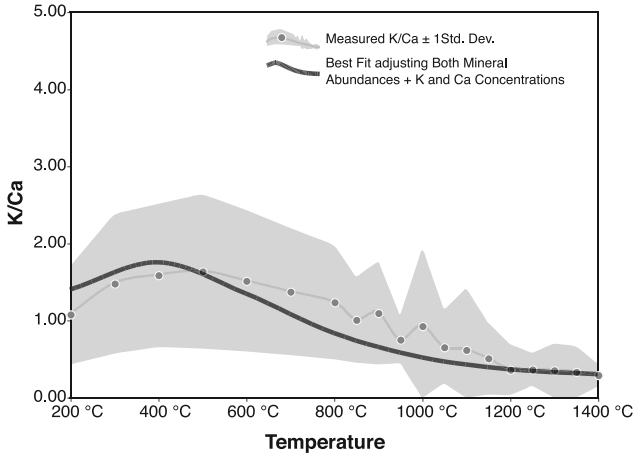

Figure 9. K/Ca best fit model results (mineralogy, Table 3; K and Ca concentrations, Table 4) and observed average values for 24 samples (medium gray line with circles) ±1 standard deviation (light gray shading). The model result (dark gray line) generally shares a similar shape and magnitude of measured K/Ca trends. The y axis is the same as K/Ca plots in Figures 3–6.

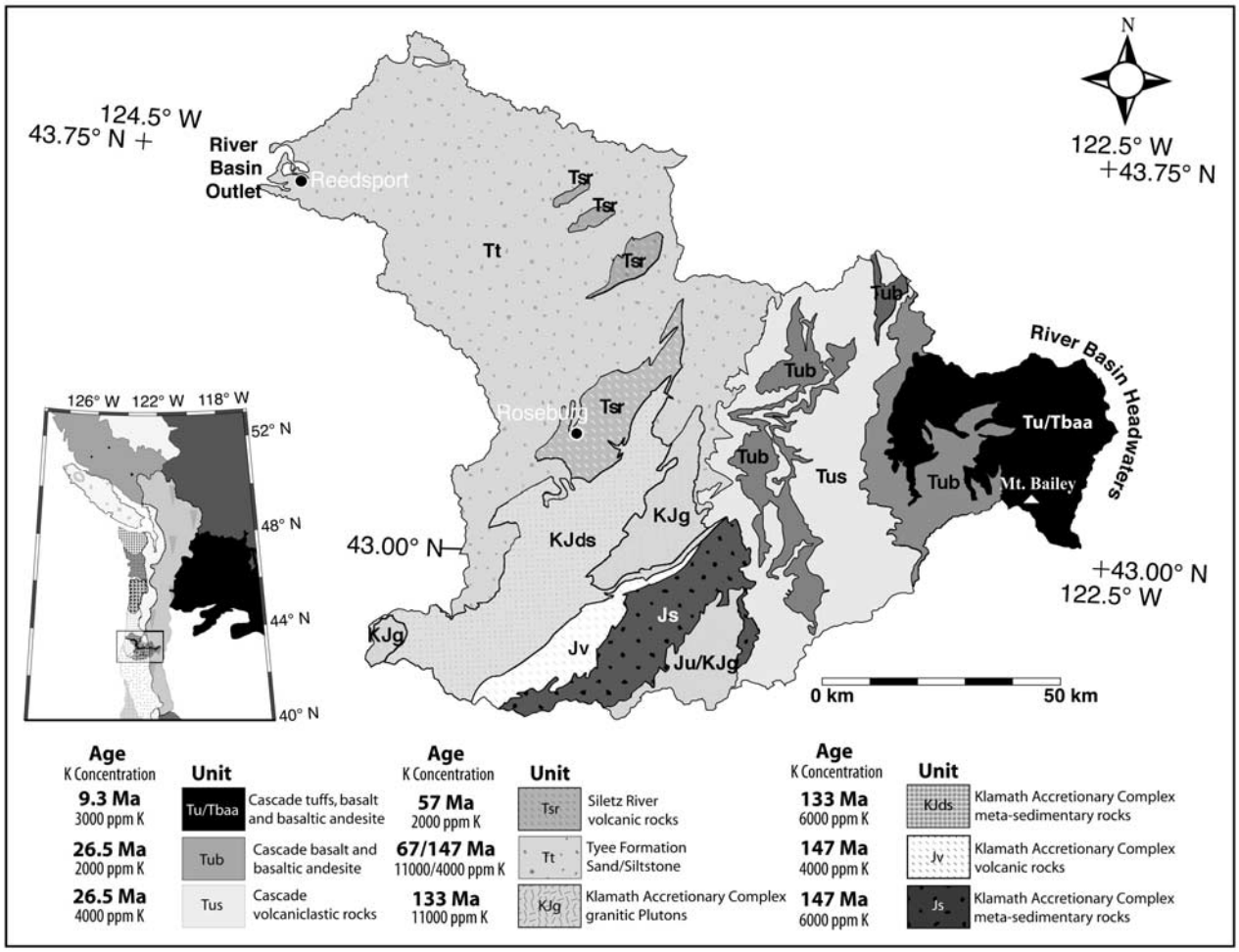

Figure 10. Umpqua River basin and simplified geology. Bulk sediment age model parameters are shown in legend (and Table 5), where ''age'' is measured or estimated crystallization age of K-bearing minerals (plagioclase and K-feldspar) and ''K concentration'' denotes either K contents of plagioclase or a mixture of plagioclase and K-feldspar. Lithologic nomenclature is after *Walker and MacLeod* [1991]. Geologic information is from *Heller et al.* [1985, 1992], *Walker and MacLeod* [1991], *Irwin and Wooden* [1999], *Wells et al.* [2000], *Barnes* [1987], and *Barnes et al.* [1986, 1992a, 1992b].

[47] The equation that expresses the weighted average age based on the parameters of K content, rock exposure area and cooling age (T_{kat}) of minerals in a given lithologic formation and ignoring differential erosion of rock types is then

$$T_{kat} = \sum_{i=1}^{n} K_i a_i t_i \div \sum_{i=1}^{n} K_i a_i$$

[48] Where n is the number of rock types, K_i is the concentration of potassium in each rock type (in ppm), a_i is outcrop area of each rock type (in km^2), and t_i is the age of each rock type (in years). We adjusted the estimated ratio of Klamath-Idaho Batholith source contributions in the Tyee Formation to their reasonable upper and lower limits (70–30% Klamath-Idaho Batholith to 30–70% Klamath-Idaho Batholith ratios) to examine model sensitivity, wherein the modeled ages were seen to vary by ±7–10 Ma in the Umpqua River basin.

7.4. Results From the Bulk Sediment ^{40}Ar-^{39}Ar Detrital Mixture Model

[49] The parameters and results for the model ages, T_{kat}, are presented in Table 5. For the Umpqua River, the modeled bulk sediment age is T_{kat} = 90 Ma (Figure 10 and Table 5), virtually identical to the average bulk sediment ^{40}Ar-^{39}Ar plateau age measured on three Umpqua River samples and within error (92 ± 7 Ma; Table 2). Even though the Rogue and Klamath Rivers erode both the Klamath Accretionary Complex and Cascade Volcanics rocks (Figures 2 and 11), their model ages are quite different. The model result for the Rogue River is T_{kat} = 128 Ma while its average bulk sediment age from four samples is identical at 129 Ma. The Klamath River model result is T_{kat} = 109 Ma, markedly different than the bulk sediment average of 151 Ma.

[50] The T_{kat} model does well in predicting the Umpqua River and Rogue River bulk sediment ages, suggesting that

Table 5. Bulk Sediment ^{40}Ar-^{39}Ar Age Model Parameters[a]

Unit[b]	Rock Type[c]	Main Minerals[d]	Whole Rock K, ppm	Area, km^2	Age, Ma	T_{kat}, Ma	^{40}Ar-^{39}Ar Age, Ma
Umpqua River Basin, Total Drainage Area of ~11,800 km^2							
Tyee Formation	ss, silt	–	–	4630	–		
Klamath Mountains Protolith	ande	plag	4000	2315	147		
Idaho Batholith Protolith	cai	plag, kspar	11,000	2315	67		
Siletz River Volcanics	bas	plag	2000	405	57		
Klamath granitic plutons	cai	plag, kspar	11,000	394	133		
KJds	ms	plag, kspar	6000	1250	147		
Jv	mmv, ande	plag	4000	297	147		
Js	ms	plag, kspar	6000	556	147		
Ju/KJg	um and cai	plag, kspar	4500	293	140		
CAS-Tus	ande	plag	4000	1850	27		
CAS-Tub	bas	plag	2000	1095	27		
CAS-Tu/Tbaa	bas-ande	plag	3000	1030	9	90	92
Total area				11,800			
Rogue River Basin, Total Drainage Area of ~13,400 km^2							
CMTT	ms	plag, kspar	6000	550	120		
WKT	um	plag	1000	2330	139		
EHT	cai, mv	plag, kspar	6000	1447	148		
ash	cai	plag, kspar	11,000	360	136		
gb	cai	plag, kspar	11,000	97	153		
gp	cai	plag, kspar	11,000	148	139		
wr	cai	plag, kspar	11,000	740	156		
w	cai	plag, kspar	11,000	54	160		
MCT	mg	plag, kspar	6000	360	156		
RCT	ims	plag	4000	820	129		
chc	cai	plag, kspar	11,000	81	157		
jo	um	plag	1000	887	161		
cs, kjds	ms	plag, kspar	6000	2490	154		
CAS	bas-ande	plag	3000	3036	21	128	129
Total area				13,400			
Klamath River Basin, Total Drainage Area of ~29,400 km^2							
rs	ss, mmv, sh	plag, kspar	6000	1918	125		
mm	cai	plag, kspar	11,000	87	400		
sb	cai	plag, kspar	11,000	320	136		
CMT	ms	plag, kspar	6000	860	135		
HF, RST	ims, mud, um, cai	plag	4000	7316	129		
ww	cai	plag, kspar	11,000	570	169		
WKT	sh, mud	plag	6000	1800	135		
wc	cai	plag, kspar	11,000	350	162		
ep	cai	plag, kspar	11,000	130	162		
NFT	cai, mv	plag, kspar	6000	1020	147		
rp	cai	plag, kspar	11,000	180	159	109	151
cc, cp, sp	cai	plag, kspar	11,000	254	136		
pl, ccr, bk, cm, cpg	mi	plag, kspar	6000	324	421		
ts	um	plag	1000	1200	136		
YT, FJT	ss, ism	plag	2000	475	159		
CAS	bas, ande	plag	3000	12,596	21	147[e]	151
Total area				29,400			

[a]K concentrations are based on the simplifications that (1) the plagioclase–K-feldspar contribution is 95–5% and (2) the K concentrations for plagioclase are 6000, 4000, 2000, and 1000 ppm for granitic plagioclase, andesitic plagioclase, basaltic plagioclase, and ultramafic plagioclase, respectively. Granitic rock units thus contribute the weighted average of 11,000 ppm K while sedimentary units that are derived from granitic units are given a more intermediate K concentration mixture of 6000 ppm. All major terranes were assigned the age of their youngest intrusion, since minerals are likely to have been reset unless metamorphic ages were available in the literature [*Wells et al.*, 2000; *Walker and MacLeod*, 1991]. Ages for the Umpqua Basin are from *Wells et al.* [2000], *Duncan* [1982], and *Heller et al.* [1985, 1992]. Note that the Umpqua River drainage area shown here is larger than published values of 9504 km^2 [*Karlin*, 1980] because of different calculation methods. Ages for the Rogue and Klamath River basins are from *Walker and MacLeod* [1991] and *Irwin and Wooden* [1999].

[b]Mapped units are as follows: Rogue and Klamath basins are from *Irwin and Wooden* [1999]. Tus, Tub, Tu, Tbaa, Tt, Tsr, KJds, KJg, Js, Jv, Ju, see Figure 10; CMTT, Condrey Mountain Terrane; WKT, Western Klamath Terrane; EHT, Eastern Hayfork Terrane; ash, Ashland Pluton; gb, Grayback pluton; gp, Grants Pass pluton; wr, White Rock pluton; w, Wimer pluton; MCT, May Creek Terrane; RST, Rattlesnake Terrane; chc, Chetco Complex; jo, Josephine Ophiolite; cs, Colebrook sediments; kjds, metasediments [*Walker and MacLeod*, 1991]; rs, redding subterrane; mm, Mule Mountain pluton, sb, Shasta Bally pluton; CMT, Central Metamorphic Terrane; HF, Hayfork terrane; ww, Wildwood pluton; WKT, Western Klamath Terrane; wc, Wooley Creek; ep, English Peak Pluton; NFT, North Fork Terrane; rp, Russian Peak pluton; cc, Canyon Creek pluton; cp, Craggy Peak Pluton, sp, Sugar Piine pluton; pl, Porcupine Lake pluton; ccr, Castle Crags pluton; bk, Bonanza King pluton; cm, China Mountain pluton; cpg, CP gabbro; YT, Yreka terrane; FJT, Fort James terrane; CAS, Cascade Volcanics.

[c]Lithologies are as follows: cai, calc-alkaline, felsic rocks; ande, andesitic; bas, basaltic; um, ultramafic rocks; mmv, mafic metavolcanics; mv, metavolcanics; mi, mafic intrusives; ss, sandstone; sh, shale; mud, mudstone; sl, slate; ms, meta-sediments; ims, interlayered metasediments.

[d]Here, plag, plagioclase; kspar, potassium feldspar.

[e]Bulk sediment age is calculated by removing the CAS (Cascade) component from the Klamath River basin (see text).

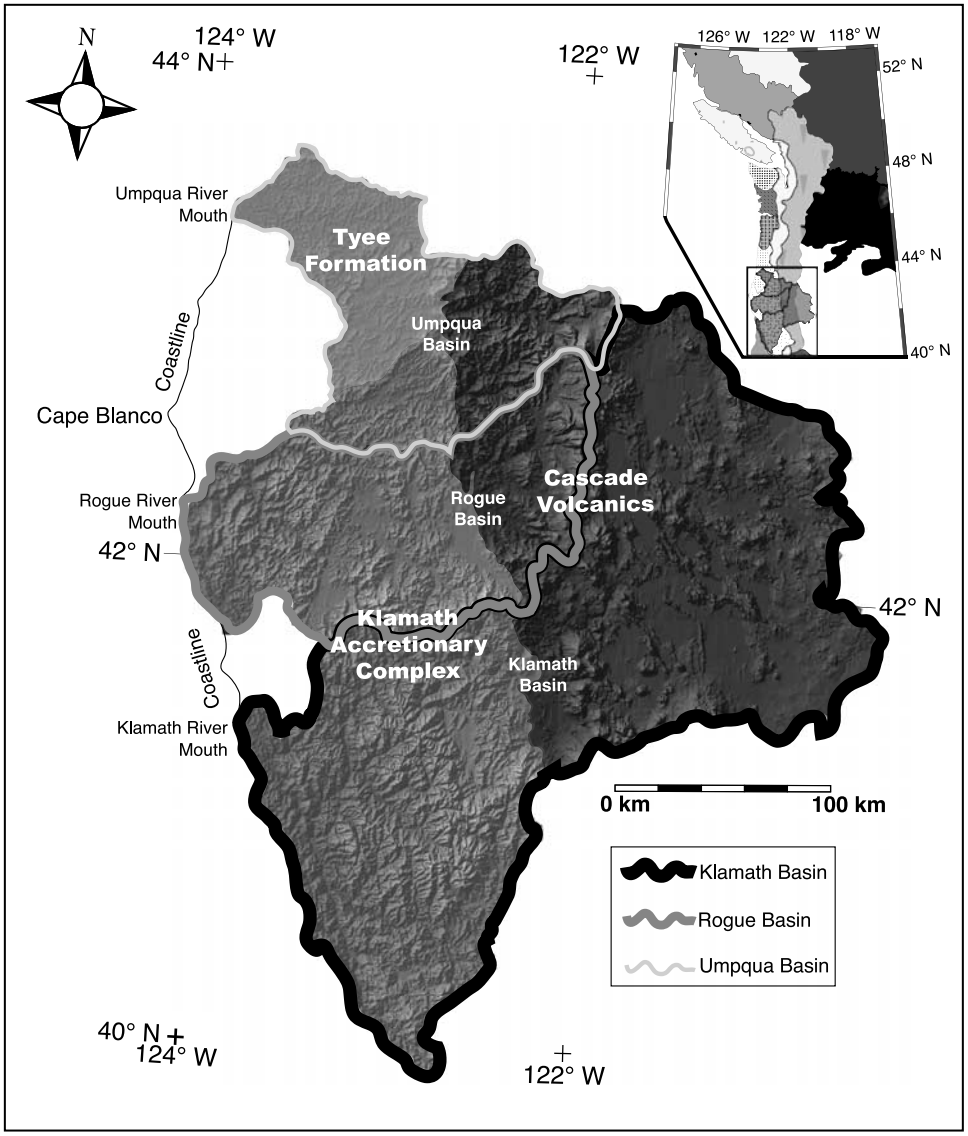

Figure 11. Shaded relief images of the Umpqua, Rogue, and Klamath River basins. Transparent geologic provinces for the Tyee Formation (light gray), the Klamath Accretionary Complex (medium gray), and the Cascade volcanic arc (dark gray) are shown. Topography of the region is characterized by moderate relief in the Tyee Formation, high relief in the Klamath Accretionary Complex, moderate to high relief in the Cascades in the headwater regions of the Umpqua and Rogue rivers, and notably low relief in the Upper Klamath basin.

the bulk sediment plateau age results can be, to a first order, faithful indicators of the weighted average cooling age of source rocks in a given basin. However, the model does not do well in the Klamath River basin and requires further examination.

8. Discussion

[51] The larger goal of this study is to characterize bulk fluvial sediment entering the northeast Pacific Ocean on a river basin scale in order to track sediment transport pathways to continental margin locations. We see distinct features in several of the large sediment contributors to the Pacific margin. Bulk sediments sampled from the mouth of the Columbia River present dual-plateau age spectra, although the age of each of the plateaus varies from sample to sample. The Klamath River, the third largest sediment producer in the Pacific Northwest also exhibits bulk sediment ages that are unique relative to other rivers in the Pacific Northwest, being the highest at 151 Ma. Rivers draining the Oregon Coast Ranges show distinct sediment plateau ages at around 88–100 Ma. Samples from the Eel River, which is presently the largest sediment producer on the Pacific margin, show age spectra that are very similar to those from the Rogue River, between 125 and 132 Ma.

[52] We show that the K/Ca spectra (and therefore the age spectra) are dominated by plagioclase feldspar and, to a lesser extent, K-feldspar. This greatly simplifies the interpretation of bulk sediment ^{40}Ar-^{39}Ar ages and we show that calculations based on a simple weighted average of source

rocks and composition suggest that the bulk sediment ages are, to a first order, faithful reflectors of provenance.

[53] Our interpretations of incremental heating-derived age spectra distinguish provenance information from Ar loss, recoil or alteration. This technique is not likely compromised by problems related to alteration and diagenesis since the step-heating procedure essentially degasses the sample from the outside inward. For the most part, the outer portion of minerals is the part that will be susceptible to chemical exchange with fluids (e.g., river water and seawater) during the weathering and transport process. Thus, by incrementally heating sediment samples, we can evaluate (through the age spectra) the extent of alteration (or the effects of Ar loss and recoil) and thus extract robust information about the source rocks from the unaltered inner portions of crystals.

8.1. Data-Model Mismatch in the Klamath Basin: Differential Erosion?

[54] The extremely low bulk detrital mixture model age for the Klamath River (109 Ma vs. the average measured bulk sediment ^{40}Ar-^{39}Ar sediment age of 151 Ma) suggests that erosional processes in the Klamath basin may not be as simply interpreted as for the Umpqua or Rogue basins. One possibility is that marked differential erosion is occurring in the Klamath basin. A population of seventy-eight U-Pb ages [*Allen et al.*, 2002] measured on zircons from sediment collected at the Klamath River mouth has an average age of 155 Ma, within error of the bulk sediment ^{40}Ar-^{39}Ar average of 151 Ma. Even though the closure temperatures are quite different for zircons and feldspars [see *Reiners et al.*, 2005b], it is reasonable to compare the two ages since both the zircon U-Pb ages and ^{40}Ar-^{39}Ar ages of minerals in our bulk sediment samples are likely related to the Mesozoic emplacement of the Klamath plutons (therefore cooling ages of the two minerals should be similar to within a few million years). Of the zircon grains measured by *Allen et al.* [2002], none had a Cascade-like signature (0–30 Ma), suggesting that material in the Cascade portion of the Klamath River basin may not contribute significantly to the sediment load found at the mouth. Notably low relief is characteristic of the topography in the upper Klamath Basin (Figure 11) when compared to both the relief in the lower Klamath basin underlain by the Klamath Accretionary Complex as well as the portion of the Umpqua and Rogue basins eroding Cascades rocks. We hypothesize that the age difference between our T_{kat} age and the measured bulk sediment age is due to a negligible amount of sediment transported out of the low-relief upper Klamath basin to the river mouth. In the extreme case where the upper Klamath basin is set to contribute no sediment to the bulk material collected at the mouth, our T_{kat} model age is 147 Ma, within error of the measured bulk sediment ^{40}Ar-^{39}Ar plateau age of 151 Ma (Table 5).

8.2. Bulk Sediment Ages in the Columbia River Sediment: Dominated by Interior Cordilleran Sources?

[55] The dual-plateau spectra observed in four out of five Columbia River samples (Figure 3) suggest that two K-bearing mineral phases of different ages, and different degassing temperature ranges influence the total ^{39}Ar released. Approximately 45% of the Columbia River drainage area consists of Northwestern Cordillera (British Columbia, Montana Rockies and the Idaho Batholith). The Columbia River Basalts (CRBs) and lavas associated with the Snake River Plain (SRP) comprise another 45% of the total basin area. Thus it is somewhat surprising that the ages presented here do not fall closer to an age in between the older, Cordilleran plutonic sources and the young Columbia River Basalt/Snake River Plain/Cascade sources. The majority of plutons comprising the Canadian portion of the upper Columbia Basin region (e.g., the Cretaceous Bayonne Magmatic Complex) are the 90–115 Ma Bayonne Suite and the 140–150 Ma Bigmouth Pluton in the Monashee, Selkirk and Purcell Mountains (Figure 2), although other Paleozoic and Early Tertiary intrusive bodies, which are less areally extensive, are present [*Ghosh*, 1995; *Logan*, 2002]. An average age weighted by mapped rock exposure area for 46 K-Ar, ^{40}Ar-^{39}Ar or U-Pb dates of plutonic bodies in southeastern British Columbia [*Logan*, 2002] is 120 Ma, which is within error of the 122 Ma average calculated from the entire set of four low-plateau and five high-plateau ages for the Columbia River sediments (Table 2).

[56] Nd isotopic analyses performed on suspended and bed load sediment from the Columbia River reflect interior, Cordilleran sources (as opposed to Cascade or Columbia River Basalt sources), supporting our ^{40}Ar-^{39}Ar bulk sediment age results. Two bed load samples have an average $\varepsilon_{Nd} = -5.5$ [*Goldstein et al.*, 1984] and a suspended sediment sample has $\varepsilon_{Nd} = -4.5$ [*Goldstein and Jacobsen*, 1988]. Since plagioclase is one of the major carriers of the rare earth elements (out of the major rock-forming minerals) and all geologic provinces in this study have similar plagioclase abundances, it might be expected that the Nd isotopic values would reflect, to some extent, a mixture of all sources in the river basin. Yet the river sediment Nd isotopic values do not reflect a mixture of Nd isotopic values from all Columbia River basin rock types (Figure 12), but values most closely resembling those of the British Columbia plutonic rocks from the Selkirk, Monashee and Purcell Mountains, which have an average $\varepsilon_{Nd} = -7.5$ [*Ghosh*, 1995], also suggesting that this region is the dominant source of sediment at the mouth of the Columbia River. It is possible, then, that the dual-plateau feature seen in the Columbia River sediment might be related to the two populations of granitic rocks mentioned above, found in the headwaters of the Columbia River basin, although this is speculative.

[57] Another perplexing finding is that we do not see strong evidence for material derived from the high-topographic-relief regions of the Idaho-Bitterroot Batholith (65–100 Ma) that are characterized by low ^{143}Nd/^{144}Nd (ε_{Nd} −10 to −20 [*Fleck*, 1990; *Mueller et al.*, 1995]) nor Cascade arc rocks which have quite young ^{40}Ar-^{39}Ar ages (0–30 Ma [*Walker and MacLeod*, 1991; *Verplanck and Duncan*, 1987]) and have ε_{Nd} values of around 4.5 (GEOROC database, available at http://georoc.mpch-mainz.gwdg.de/georoc/). This is somewhat surprising considering that erosion rates are often greater in high-relief regions [*Ahnert*, 1970; *Burbank et al.*, 2003], or in regions experiencing high rates of rock uplift [*Wobus et al.*, 2003] or precipitation [*Reiners et al.*, 2003]. Both regions comprise only about 8% each of the total area for the Columbia River catchment, which helps explain why the signatures of these geologic provinces are not seen in our analyses. However,

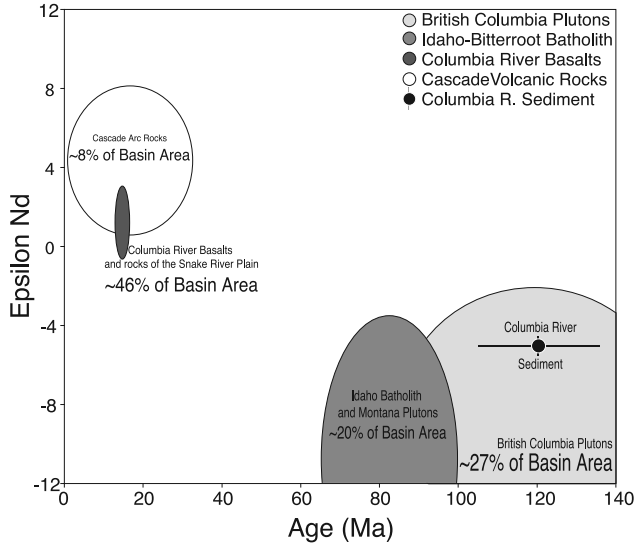

Figure 12. Nd isotopes (ε_{Nd}) versus cooling/crystallization age or, in the case of the Columbia River, bulk sediment ^{40}Ar-^{39}Ar plateau age. Data sources are as follows: Canadian plutons are from *Ghosh* [1995] and *Logan* [2002]; Idaho Batholith data are from *Foster et al.* [2001] and *Fleck* [1990]; Columbia River Basalt and Cascade arc data are from GEOROC (http://georoc.mpch-mainz.gwdg.de/georoc/); Columbia River Nd isotopic data and error are from *Goldstein et al.* [1984] and *Goldstein and Jacobsen* [1988]. As discussed in the text, the Columbia River sediment most closely resembles the intrusive rocks from British Columbia.

considering how proximal the high-relief Cascades are to the mouth of the Columbia River and the fact that notable erosion is occurring there [*Reiners et al.*, 2003] this explanation is not entirely satisfactory. Likewise, *Reiners et al.* [2005a] saw little evidence for a Cascade signature from zircon analyses of Tertiary-age fluvial-derived sandstones in the Olympic Mountains, in spite of the fact that sediments comprising the units had to have been transported through the paleo-Cascades. This may indicate that the Cascades do not contribute a significant amount of sediment to the larger size fractions. Minerals from fine-grained volcanic rocks may break down to smaller size fractions (<20 μm) more easily/faster (relative to plutonic minerals) during erosion, producing a size fraction bias. It has been suggested that volcanic rocks break down by chemical weathering up to 50 times more quickly than granites [*Drever and Clow*, 1995]. Thus Cascade and other volcanic rocks in these catchments may be underrepresented in silt-sized material and be more preferentially reflected through clays and the solute load. It has been shown that minerals related to granitic rocks like micas, K-feldspars and sodic to intermediate plagioclase are the longest-lasting detrital minerals, while hornblende and calcic plagioclase have an order-of-magnitude shorter lifetime [*Kowalewski and Rimstidt*, 2003]. These findings suggest that minerals comprising the sediment at the mouths of the Columbia, Rogue and Klamath Rivers, for example, could show bias to older, plutonic sources. An alternative explanation to these data is that high relief alone is not enough to dictate how much erosion is occurring in the different geologic provinces. Higher rates of rock uplift or precipitation may also be playing a role and this provides an area for future research.

8.3. Other Considerations

[58] As noted earlier, loss of radiogenic ^{40}Ar and recoil of ^{39}Ar and ^{37}Ar can affect ^{40}Ar-^{39}Ar analyses. We see strong evidence for both. ^{40}Ar loss appears to be a consistent feature in almost all of the samples. The loss is generally confined to the lower-temperature steps, where the less retentive minerals or the weathered margins of more retentive minerals are degassing. What is surprising is that ^{40}Ar loss is not much more pervasive, considering that most of the minerals in these sediments come from surface outcrops that are exposed to chemical weathering and have been mechanically broken down during transport. One possible explanation to this is that the physical weathering process removes the less retentive, altered and fractured outer edges, and leaves behind more pristine mineral crystals.

[59] Ar recoil is most consistently observed in samples that drain the Tertiary Tyee Formation (Coos and Umpqua Rivers) and Mesozoic Franciscan Melange (the Eel, Mattole and Russian Rivers). Both of these sediment formations are composed of mineral particles that are sourced from Mesozoic protoliths, suggesting that recoil is common in material derived from old sedimentary rocks; possibly because of diagenetic factors compounded by exposure to more physical and chemical weathering (e.g., these minerals and rock fragments have been through the weathering process at least twice).

[60] Some of the estuary samples did not provide ages that were reproducible. Since tides and longshore currents often bring material into the estuary it was important to avoid sampling near the mouth [*Peterson et al.*, 1982]. Yet we now see that any sample taken further inland in an estuary with complex hydrography, away from tidally derived beach material, is not always representative of what enters the ocean, as evidenced by the wide range in ages from samples taken from the Tillamook and Willapa estuaries. However, this should only be true in cases where several major rivers feed into one estuary, and is dependent on the shape of the estuary and the distribution of erodable rock types in the contributing drainage area [*Peterson et al.*, 1984]. The bulk sediment ^{40}Ar-^{39}Ar ages from Willapa Bay (WIL-2 and 4) and Tillamook Bay (TIL-1 and 2) are unlikely to be fully homogenized (well mixed) and therefore do not provide a reliable ^{40}Ar-^{39}Ar fingerprint.

[61] The K/Ca spectra provide important insights into the composition of our bulk samples but generally do not provide much in the way of diagnostic provenance information since K/Ca values are seen to change through the step-heating process for different samples from the same river. The reasons for this are likely related to variable mineralogy, variable contributions of minerals to the plateau portion of the age spectra and ^{39}Ar loss in the reactor. When compared with ICP-OES K/Ca ratios, systematically lower Ar-derived integrated K/Ca values are observed in samples that have very low initial K/Ca values in their spectra (for example, COO-1A, Figure 4; ROG-5, Figure 5; RUS-2, Figure 6). The most plausible explanation for this difference is reactor-related loss of ^{39}Ar (i.e., K), which results in K/Ca measurements that are unexpectedly low and not truly

representative of the mineralogy at the lower temperature steps. The K/Ca spectra acquired during the middle- and high-temperature steps, however, reflect real differences in mineralogy.

[62] Finally, we acknowledge that other important factors dictating the flux and types of sediment delivered through the fluvial system, such as anomalous storms, mass wasting events, fires, logging, agricultural practices and river diversion projects, are not considered here because of the difficulty in addressing these problems in the framework of longer-term, geological cycles and regional scales.

9. Conclusions and Implications

[63] This paper highlights a new method that characterizes bulk sediment for provenance studies using the ^{40}Ar-^{39}Ar incremental heating technique. We analyzed the 20–63 μm size fraction of bulk river sediments from the mouths of 14 Pacific Northwest rivers for the purpose of identifying sources and examining the feasibility of using bulk sediment ^{40}Ar-^{39}Ar plateau ages and age spectra patterns to track the contributions of specific rivers to continental margin sedimentation. We examined the silt-sized material since this fraction contains mostly rock-forming minerals and yet it is small enough to be transported to most continental margin sediment sites via ocean currents. Significant findings are as follows:

[64] 1. Reproducible age spectra provide robust ''fingerprints'' for many individual rivers in the Pacific Northwest, both by the shape of the age spectra and by the bulk sediment ^{40}Ar-^{39}Ar plateau ages. Major problems in this data set appear to be related to sampling bias and not the technique itself (for instance, variability in age spectra seen in samples from large estuaries are related to nonhomogenization of several river sources in a complex estuarine system).

[65] 2. A K/Ca degassing model is developed to test, in light of bulk mineralogy and diffusion of silicates, whether measured K/Ca spectra (determined from ^{39}Ar and ^{37}Ar) are reasonable indicators of contributing minerals, given typical K and Ca compositions. The model shows that the bulk mineralogy is reflected in the outgassing K/Ca spectra and that plagioclase is likely to be the dominant mineral producing the age plateaus, followed by K-feldspar.

[66] 3. A basin-scale ''weighted average cooling age'' model is also developed to test the consistency of our measured bulk sediment plateau ages with known source rock age and compositions. The simple model takes into account K content (of plagioclase and K-feldspar), cooling age and areal extent of geologic units to predict bulk sediment plateau ages for the Umpqua, Rogue and Klamath river basins. The Umpqua basin model prediction is 90 Ma, very similar to the average bulk sediment ^{40}Ar-^{39}Ar age (92 Ma). The model predicted 128 Ma for the Rogue River, virtually identical to the average bulk sediment age of 129 Ma calculated from four ^{40}Ar-^{39}Ar analyses. The modeled age for the Klamath River is 109 Ma, considerably younger than the average bulk sediment age of 151 Ma. However, if we include the effect of differential erosion occurring in the high-relief Klamath Mountain and low-relief Cascades and/or transport of this material to the mouth, a model age of 147 Ma is predicted.

[67] 4. Results from the Klamath and Rogue Rivers, which drain the same lithologic formations, show distinct ^{40}Ar-^{39}Ar bulk sediment plateau ages, highlighting the fact that this technique has the power to resolve sediment sources on a drainage basin scale. These results also suggest that in cases where ''fingerprints'' are the goal, this method shows promise to be as diagnostic as single-grain methods (e.g., ^{40}Ar-^{39}Ar age determinations on mica and K-feldspar, U-Pb age measurements on zircons, etc.) often used in fluvial settings. For example, the Rogue and Klamath Rivers likely contain differing proportions of single grain populations in which a large number of analyses would be necessary to resolve differences statistically. However, these differing proportions of rock types contributing detrital minerals to the fluvial sediment can be resolved with very few measurements using incremental heating on bulk sediment. Future work involving the coupling of single-grain analyses with this bulk sediment ^{40}Ar-^{39}Ar incremental heating method will further refine the technique and will also expand its utility.

[68] 5. On the basis of Nd isotopic analyses [*Goldstein and Jacobsen*, 1988; *Goldstein et al.*, 1984] in conjunction with our bulk sediment age results, we infer that the Columbia River sediment is dominated by detrital minerals from Canadian Cordilleran rocks. It is interesting that Cascade rocks seem to be ''missing'' in measurements made on the bed load sediment (both data presented here and that of *Goldstein et al.* [1984] and *Goldstein and Jacobsen* [1988]) of the Columbia River even though notable erosion occurs there [*Reiners et al.*, 2003]. This observation has been made before for much older fluvial-derived sediments in the Pacific Northwest [*Reiners et al.*, 2005a] and may be related to a combination of grain size differences between plutonic and volcanic minerals and the rates at which these minerals break down. The information unraveled by the ^{40}Ar-^{39}Ar method presented here coupled with the few Nd isotopic analyses from the Columbia River [*Goldstein and Jacobsen*, 1988; *Goldstein et al.*, 1984] suggests that the two isotopic systems could prove to be a powerful combination in not only identifying provenance but also unraveling erosion dynamics on large fluvial basin scales.

[69] Our results show promise for applying this technique to a variety of climatic and tectonic problems. These include delineating downcore provenance change on fluvial basin scales to unravel trends in oceanographic circulation and sediment fluxes through geologic time. Because the technique captures information about weathering and alteration, it may also be well suited to contrast physical vs. chemical weathering in terrigenous sediments. It could also be a valuable tool for understanding both spatial and temporal changes in basin hydrology related to natural climate and tectonic cycles over geologic timescales.

[70] The inferences made by the ''average cooling age'' model suggest that there may also be a future for this technique in the realm of tectonic geomorphology and thermochronology at continental margin sites where single-grain analyses are not feasible. Although bulk sediment is inherently complex, the findings presented here show that quantitative information about provenance and erosion can be extracted from ^{40}Ar-^{39}Ar heating of polymineralic materials, and suggest that this method has broad application to doc-

umenting tectonic and climatic processes through the tracking of fine-grained terrigenous material.

[71] **Acknowledgments.** We thank Robert Anderson, Alex Densmore, Peter Clift, and an anonymous reviewer for their efforts in making this manuscript much better. Many thanks to John Huard for analytical, technical, and intellectual contributions throughout the project, Andy Ungerer and Mysti Weber for sample preparation guidance, Dave Graham and Adam Kent for help solidifying many of the ideas found in this paper, Bill Rugh for technical assistance, Charlotte Allen for sharing U-Pb zircon analyses from the Klamath River, Mark Harrison for a short, yet poignant discussion that improved this work, Matt Coble, Claire Schuft, and Moya Duncan for help with sample preparation, Chris Russo for intellectual stimulation over the course of this work, Andrew Meigs, and COAS. This research was funded by NSF grant ATM0135294.

References

Ahnert, F. (1970), Functional relationships between denudation, relief, and uplift in large mid-latitude basins, *Am. J. Sci.*, *268*, 243–263.

Allen, C. M., C. G. Barnes, and I. H. Campbell (2002), U-Th-Pb ages from Klamath River detrital zircons using LA-ICP-MS, *Geol. Soc. Am. Abstr. Programs*, *34*, 434.

Barnes, C. G. (1987), Mineralogy of the Wooley Creek batholith, Slinkard pluton and related dikes, Klamath Mountains, northern California, *Am. Mineral.*, *72*, 879–901.

Barnes, C. G., J. M. Rice, and R. F. Gribble (1986), Tilted plutons in the Klamath Mountains of California and Oregon, *J. Geophys. Res.*, *91*, 6059–6071.

Barnes, C. G., M. A. Barnes, and R. W. Kistler (1992a), Petrology of the Caribou Mountain Pluton, Klamath Mountains, California, *J. Petrol.*, *33*, 95–124.

Barnes, C. G., S. W. Petersen, R. W. Kistler, T. Prestvik, and B. Sundvoll (1992b), Tectonic implications of isotopic variation among Jurassic and Early Cretaceous plutons, Klamath Mountains, *Geol. Soc. Am. Bull.*, *104*, 117–126.

Bernet, M., M. T. Brandon, J. I. Garver, and B. Molitor (2004), Fundamentals of detrital zircon fission-track analysis for provenance and exhumation studies with examples from the European Alps, in *Detrital Thermochronology: Provenance Analysis, Exhumation and Landscape Evolution of Mountain Belts*, edited by M. Bernet and C. Spiegel, *Spec. Pap. Geol. Soc. Am.*, *378*, 25–36.

Blake, M. C., and D. L. Jones (1981), The Franciscan melange in northern California: A reinterpretation, in *The Geotectonic Evolution of California*, edited by W. G. Ernst, pp. 306–328, Prentice Hall, Upper Saddle River, N. J.

Brady, J. B. (1995), Diffusion data for silicate minerals, glasses and liquids, in *A Handbook of Physical Constants: Mineral Physics and Crystallography*, *AGU Ref. Shelf Ser.*, vol. 2, edited by T. J. Ahrens, pp. 269–290, AGU, Washington D. C.

Brandon, M. T., and J. A. Vance (1992), Tectonic evolution of the Cenozoic Olympic subduction complex, Washington state, as deduced from fission track ages for detrital zircons, *Am. J. Sci.*, *292*, 565–636.

Burbank, D. W., A. E. Blythe, J. Putkonen, B. Pratt-Sitaula, E. Gabet, M. Oskin, A. P. Barros, and T. P. Ojha (2003), Decoupling of erosion and precipitation in the Himalayas, *Nature*, *426*, 652–655.

Carrapa, B., J. Wijbrams, and G. Bertolli (2004), Detecting provenance variations and cooling patterns within the weestern Alpine orogen through $^{40}Ar/^{39}Ar$ geochronology on detrital sediments: The Tertiary Piedmont Basin, northwest Italy, in *Detrital Thermochronology: Provenance Analysis, Exhumation, and Landscape Evolution of Mountain Belts*, edited by M. Bernet and C. Spiegel, *Spec. Pap. Geol. Soc. Am.*, *378*, 67–103.

Carter, A. (1999), Present status and future avenues of source region discrimination and characterization using fission track analyses, *Sediment. Geol.*, *124*, 31–45.

Clift, P. D., and J. Blusztajn (2005), Reorganization of the western Himalaya river system after five million years ago, *Nature*, *438*, 1001–1003.

Clift, P. D., N. Shimizu, G. D. Layne, and J. Blusztajn (2001), Tracing patterns of erosion and drainage in the Paleogene Himalaya through ion probe Pb isotope analysis of detrital K-feldspars in the Indus Molasse, India, *Earth Planet. Sci. Lett.*, *188*, 475–491.

Clift, P. D., J. I. Lee, P. Hildebrand, N. Shimizu, G. D. Layne, J. D. Blum, E. Garzanti, and A. A. Khan (2002), Nd and Pb isotope variability in the Indus River system: Implications for crustal heterogeneity in the Western Himalaya, *Earth Planet. Sci. Lett.*, *200*, 91–106.

Clift, P. D., I. H. Campbell, M. S. Pringle, A. Carter, X. Zhang, K. V. Hodges, A. A. Khan, and C. M. Allen (2004), Thermochronology of the modern Indus River bedload: New insight into the controls on the marine stratigraphic record, *Tectonics*, *23*, TC5013, doi:10.1029/2003TC001559.

Copeland, P., M. Harrison, and M. T. Heizler (1990), $^{40}Ar/^{39}Ar$ single-crystal dating of detrital muscovite and K-feldspar from Leg 116, southern Bengal Fan: Implications for the uplift and erosion of the Himalayas, *Proc. Ocean Drill. Program Sci. Results*, *116*, 93–114.

Dalrymple, G. B., and M. A. Lanphere (1969), *Potassium-Argon Dating: Principles, Techniques and Applications to Geochronology*, 258 pp., W. H. Freeman, New York.

Dalrymple, G. B., E. C. Alexander Jr., M. A. Lanphere, and G. P. Kraker (1981), Irradiation of samples for $^{40}Ar/^{39}Ar$ dating using the Geological Survey TRIGA reactor, *U. S. Geol. Surv. Prof. Pap.*, *1176*, 55 pp.

Darby, D. A. (2003), Sources of sediment found in sea ice from the western Arctic Ocean: New insights into processes of entrainment and drift patterns, *J. Geophys. Res.*, *108*(C8), 3257, doi:10.1029/2002JC001350.

Deer, W. A., R. A. Howie, and J. Zussman (1992), *An Introduction to Rock-Forming Minerals*, 2nd ed., 696 pp., John Wiley, Hoboken, N. J.

Dong, H., C. M. Hall, D. R. Peacor, and A. N. Halliday (1995), Mechanisms of argon retention in clays revealed by laser ^{40}Ar-^{39}Ar dating, *Science*, *267*, 355–359.

Drever, J. I., and D. W. Clow (1995), Weathering rates in catchments, in *Chemical Weathering Rates in Silicate Minerals*, edited by A. F. White and S. L. Brantley, pp. 463–481, Mineral. Soc. of Am., Washington, D. C.

Duncan, R. A. (1982), A captured island chain in the Coast Range of Oregon and Washington, *J. Geophys. Res.*, *87*, 10,827–10,837.

Fagel, N., C. Innocent, R. Stevenson, C. Gariepy, and C. Hillaire-Marcel (1996), A high resolution Nd and Pb isotopic study of Labrador Sea clays at the 2/1 transition; implications for sedimentary supplies and deep circulation changes, *Eos Trans. AGU*, *77*(46), Fall Meet. Suppl., F324.

Fagel, N., C. Innocent, C. Gariepy, and C. Hillaire-Marcel (2002), Sources of Labrador Sea sediments since the last glacial maximum inferred from Nd-Pb isotopes, *Geochim. Cosmochim. Acta*, *66*, 2569–2581.

Faure, G. (1986), *Principles of Isotope Geology*, John Wiley, Hoboken, N. J.

Fechtig, H., and S. Kalbitzer (1966), The diffusion of argon in potassium-bearing solids, in *Potassium Argon Dating*, edited by O. E. Schaeffer and J. Zahringer, pp. 68–107, Springer, New York.

Fleck, R. J. (1990), Neodymium, strontium and trace-element evidence of crustal anatexis and magma mixing in the Idaho Batholith, in *The Nature and Origin of Cordilleran Magmatism*, edited by J. L. Anderson, *Mem. Geol. Soc. Am.*, *174*, 359–373.

Foster, D. A., C. Schafer, C. M. Fanning, and D. W. Hyndman (2001), Relationships between crustal melting, plutonism, orogeny, and exhumation: Idaho-Bitterroot batholith, *Tectonophysics*, *342*, 313–350.

Fox, K. J., R. J. Fleck, G. H. Curtis, and C. E. Meyer (1985), Implications for the northwesterdly younger age of the volcanic rocks of west-central California, *Geol. Soc. Am. Bull.*, *96*, 647–654.

Garzanti, E., S. Critelli, and R. V. Ingersoll (1996), Paleogeographic and paleotectonic evolution of the Himalayan Range as reflected by detrital modes of Tertiary sandstones and modern sands (Indus transect, India and Pakistan), *Geol. Soc. Am. Bull.*, *108*, 631–642.

Garzanti, E., G. Vezzoli, S. Andò, P. Paparella, and P. D. Clift (2005), Petrology and mineralogy of Indus River sands: A key to interpret erosion history of the Western Himalayan Syntaxis, *Earth Planet. Sci. Lett.*, *229*, 287–302.

Ghosh, D. (1995), Nd-Sr isotopic constraints on the interactions of the intermontane Superterrane with the western edge of North America in the southern Canadian Cordillera, *Can. J. Earth Sci.*, *32*, 1740–1758.

Gillespie, A. R., J. C. Huneke, and G. J. Wasserburg (1982), An assessment of ^{40}Ar-^{39}Ar dating of incompletely degassed xenoliths, *J. Geophys. Res.*, *87*, 9247–9257.

Goldstein, S. L., and S. B. Jacobsen (1988), Nd and Sr isotopic systematics of river water suspended material: Implications for crustal evolution, *Earth Planet. Sci. Lett.*, *87*, 249–265.

Goldstein, S. L., R. K. O'Nions, and P. J. Hamilton (1984), A Sm-Nd isotopic study of atmospheric dusts and particulates from major river systems, *Earth Planet. Sci. Lett.*, *70*, 221–236.

Harrison, T. M., I. Duncan, and I. McDougall (1985), Diffusion of ^{40}Ar in biotite: Temperature, pressure and compositional effects, *Geochim. Cosmochim. Acta*, *49*, 2461–2468.

Heller, P. L., Z. E. Peterman, J. R. O'Neil, and M. Shafiqullah (1985), Isotopic provenance of sandstones from the Eocene Tyee Formation, Oregon Coast Range, *Geol. Soc. Am. Bull.*, *96*, 770–780.

Heller, P. L., P. R. Renne, and J. R. O'Neil (1992), River mixing rate, residence time, and subsidence rates from isotopic indicators: Eocene snadstones from the U.S. Pacific Northwest, *Geology*, *20*, 1095–1098.

Hemming, S. R., W. S. Broecker, W. D. Sharp, G. C. Bond, R. H. Gwiazda, J. F. McManus, M. Klas, and I. Hajdas (1998), Provenance of Heinrich layers in core V28–82, northeastern Atlantic: $^{40}Ar/^{39}Ar$ ages of ice-rafted

hornblende, Pb isotopes in feldpar grains, and Nd-Sr-Pb isotopes in the fine sediment fraction, *Earth Planet. Sci. Lett.*, *164*, 317–333.

Hemming, S. R., C. M. Hall, S. M. Biscaye, S. Higgins, G. C. Bond, J. F. McManus, D. C. Barber, J. T. Andrew, and W. S. Broecker (2002), $^{40}Ar/^{39}Ar$ ages and ^{40}Ar* concentrations of fine-grained sediment fractions from North Atlantic Heinrich layers, *Chem. Geol.*, *182*, 583–603.

Howard, A. D. (1998), Long profile development of bedrock channels: Interaction of weathering, mass wasting, bed erosion and sediment transport, in *Rivers Over Rock: Fluvial Processes in Bedrock Channels*, *Geophys. Monogr. Ser.*, vol. 107, edited by K. J. Tinkler and E. E. Wohl, pp. 297–319, AGU, Washington, D. C.

Howard, A. D., M. A. Siedl, and W. E. Dietrich (1994), Modeling fluvial erosion on regional to continental scales, *J. Geophys. Res.*, *99*, 13,971–913,986.

Irwin, W. P. (1997), Preliminary map of selected post-Nevadan geologic features of the Klamath Mountains and adjacent areas, California and Oregon, *U. S. Geol. Surv. Open File Rep., 97-465*, 29 pp.

Irwin, W. P., and J. L. Wooden (1999), Plutons and accretionary episodes of the Klamath mountains, California and Oregon, *U.S. Geol. Surv. Open File Rep., 99-374*.

Jantschik, R., and S. Huon (1992), Detritial silicates in northeast Atlantic deep-sea sediments during the Late Quaternary: Mineralogical and K-Ar isotopic data, *Eclogae Geol. Helv.*, *85*, 195–212.

Karlin, R. (1980), Sediment sources and clay mineral distributions off the Oregon coast, *J. Sediment. Petrol.*, *50*, 543–560.

Koppers, A. P. (2002), ArArCalc: Software for $^{40}Ar/^{39}Ar$ age calculations, *Comput. Geosci.*, *28*, 605–619.

Kowalewski, M., and J. D. Rimstidt (2003), Average lifetime and age spectra of detrital grains: Toward a unifying theory of sedimentary particles, *J. Geol.*, *111*, 427–439.

Kuhlemann, J., W. Frisch, I. Dunkl, M. Kazmer, and Schmiedl (2004), Miocene siliciclastic deposits of Naxos Island: Geodynamic and environmental implications for the evolution of the southern Aegean Sea (Greece), in *Detrital Thermochronology: Provenance Analysis, Exhumation, and Landscape Evolution of Mountain Belts*, edited by M. Bernet and C. Spiegel, *Spec. Pap. Geol. Soc. Am.*, *378*, 51–65.

Lamy, F., D. Hebbeln, and G. Wefer (1998), Late Quaternary precessional cycles of terrigenous sediment input off the Norte Chico (27.5°S) and paleoclimatic implications, *Paleogeogr. Paleoclim. Paleoecol.*, *141*, 233–251.

Lamy, F., D. Hebbeln, and G. Wefer (1999), High resolution marine record of climatic change in mid-latitude Chile during the last 28 ka based on terrigenous sediment parameters, *Quat. Res.*, *51*, 83–93.

Lisitzin, A. P. (1996), *Oceanic Sedimentation: Lithology and Geochemistry*, 399 pp., AGU, Washington, D. C.

Logan, J. M. (2002), Intrusion related mineral occurrences of the Cretaceous Bayonne Magmatic Belt, southeast British Columbia, *Geosci. Map 2002-1*, scale 1:500,000, Geol. Surv. Branch, Victoria, B.C., Canada.

Lovera, O. M., M. Grove, T. M. Harrison, and K. I. Mahon (1997), Systematic analysis of K-feldspar $^{40}Ar/^{39}Ar$ step heating results: I. Significance of activation energy determinations, *Geochim. Cosmochim. Acta*, *61*, 3171–3192.

McDougall, I., and T. M. Harrison (1999), *Geochronology and Thermochronology by the $^{40}Ar/^{39}Ar$ Method*, 269 pp., Oxford Univ. Press, New York.

McLaughlin, R. J., W. V. Sliter, N. O. Fredriksen, W. P. Harbert, and D. S. McCulloch (1994), Plate motions recorded in tectonostratigraphic terranes of the Franciscan Complex and evolution of the Mendocino Triple Junction, northwestern California, *U.S. Geol. Surv. Bull., 1997*, 60 pp.

Monger, J. W., R. A. Price, and D. J. Templeman-Kluit (1982), Tectonic accretion and the origin of the two major metamorphic and plutonic belts in the Canadian Cordillera, *Geology*, *10*, 70–75.

Montgomery, D. R. (1994), Valley incision and the uplift of mountain peaks, *J. Geophys. Res.*, *99*, 13,913–13,921.

Mueller, P. A., R. D. Shuster, K. A. D'Arcy, A. L. Heatherington, A. P. Nutman, and I. S. Williams (1995), Source of the northeast Idaho Batholith: Isotopic evidence for a Paleoproterozoic terrane in the northwestern U.S., *J. Geol.*, *103*, 63–72.

Peterson, C., K. F. Scheidegger, and P. Komar (1982), Sand-dispersal patterns in an active-margin estuary of the northwestern United States as indicated by sand composition, texture and bedforms, *Mar. Geol.*, *50*, 77–96.

Peterson, C., K. Scheidegger, P. Komar, and W. Niem (1984), Sediment composition and hydrography in six high-gradient estuaries of the northwestern United States, *J. Sediment. Petrol.*, *54*, 86–97.

Pettke, T., A. N. Halliday, C. M. Hall, and D. K. Rea (2000), Dust production and deposition in Asia and the North Pacific Ocean over the past 12 Myr, *Earth Planet. Sci. Lett.*, *178*, 397–413.

Pisias, N. G., A. C. Mix, and L. Heusser (2001), Millennial scale climate variability of the northeast Pacific Ocean and northwest North America based on radiolaria and pollen, *Quat. Sci. Rev.*, *20*, 1561–1576.

Reiners, P. W., T. A. Ehlers, S. G. Mitchell, and D. W. Montgomery (2003), Coupled spatial variations in precipitation and long-term erosion rates across the Washington Cascades, *Nature*, *426*, 645–647.

Reiners, P. W., I. H. Campbell, S. Nicolescu, C. M. Allen, J. K. Hourigan, J. I. Garver, J. M. Mattinson, and D. S. Cowan (2005a), (U-Th)/(He-Pb) Double dating of detrital zircons, *Am. J. Sci.*, *305*, 259–311.

Reiners, P. W., T. A. Ehlers, and P. K. Zeitler (2005b), Past, present, and future of thermochronology, *Rev. Mineral. Geochem.*, *58*, 1–18.

Renne, P. R., A. L. Deino, R. C. Walter, B. D. Turrin, C. C. Swisher, T. A. Becker, G. H. Curtis, W. D. Sharp, and A.-R. Jaouni (1994), Intercalibration of astronomical and radioisotopic time, *Geology*, *22*, 783–786.

Ryu, I., and A. R. Niem (1999), Sandstone diagenesis, reservoir potential and sequence stratigraphy of the Eocene Tyee Basin, Oregon, *J. Sediment. Res.*, *69*, 384–393.

Spiegel, C., W. Siebel, J. Kuhlemann, and W. Frisch (2004), Toward a comprehensive provenance analysis: A multi-method approach and its implications for the evolution of the Central Alps, in *Detrital Thermochronology: Provenance Analysis, Exhumation, and Landscape Evolution of Mountain Belts*, edited by M. Bernet and C. Spiegel, *Spec. Pap. Geol. Soc. Am.*, *378*, 37–50.

Turner, G., and P. H. Cadogan (1974), Possible effects of ^{39}Ar recoil in ^{40}Ar-^{39}Ar dating, *Geochim. Cosmochim. Acta*, *5*, 1601–1615.

Verplanck, E. P., and R. A. Duncan (1987), Temporal variations in plate convergence and eruption rates in the Western Cascades, Oregon, *Tectonics*, *6*, 197–209.

Walczak, P. W. (2006), Submarine plateau volcanism and Cretaceous Ocean Anoxic Event 1a: Geochemical evidence from Aptian sedimentary sections, M.S. thesis, 172 pp., Coll. of Ocean and Atmos. Sci., Oreg. State Univ., Corvallis.

Walker, G. W., and N. S. MacLeod (1991), Geologic map of Oregon, scale 1:500,000, U.S. Geol. Surv., Denver, Colo.

Walter, H. J., E. Hegner, B. Diekmann, G. Kuhn, and M. M. Rutgers van der Loeff (2000), Provenance and transport of terrigenous sediment in the South Atlantic Ocean and their relations to glacial and interglacial cycles: Nd and Sr isotopic evidence, *Geochim. Cosmochim. Acta*, *64*, 3813–3827.

Wang, S., I. McDougall, N. Tetley, and T. M. Harrison (1980), $^{40}Ar/^{39}Ar$ age and thermal history of the Kirin Chondrite, *Earth Planet. Sci. Lett.*, *49*, 117–131.

Wells, R. E., A. S. Jayko, A. R. Niem, G. Black, T. Wiley, E. Baldwin, K. M. Molenaar, K. L. Wheeler, C. B. DuRoss, and R. W. Givler (2000), Geologic map and database of the Roseburg 30 × 60 quadrangle, Douglas and Coos counties, Oregon, *U.S. Geol. Surv. Open File Rep., 00-376*.

Wendt, I., and C. Carl (1991), The statistical distribution of the mean standard weighted deviation, *Chem. Geol.*, *86*, 275–285.

Whipple, K. X., and G. E. Tucker (1999), Dynamics of the stream-power river incision model: Implications for height limits of mountain ranges, landscape response timescales, and research needs, *J. Geophys. Res.*, *104*, 17,661–17,674.

Whipple, K. X., E. Kirby, and S. H. Brocklehurst (1999), Geomorphic limits to climate-induced increases in topographic relief, *Nature*, *401*, 39–43.

Wobus, C. W., K. V. Hodges, and K. X. Whipple (2003), Has focused denudation sustained active thrusting at the Himalayan topographic front?, *Geology*, *31*, 861–864.

Zhang, G., J. T. Germaine, R. T. Martin, and A. J. Whittle (2003), A simple sample-mounting method for random powder X-ray diffraction, *Clays Clay Miner.*, *51*, 218–225.

R. A. Duncan, N. G. Pisias, and S. VanLaningham, College of Oceanic and Atmospheric Sciences, Oregon State University, 104 COAS Administration Building, Corvallis, OR 97331, USA. (svanlani@coas.oregonstate.edu)